

Buckling behaviour of single-walled nanotubes

By

Ghata P.Tiwari

(15MMCC05)



DEPARTMENT OF MECHANICAL ENGINEERING
INSTITUTE OF TECHNOLOGY
NIRMA UNIVERSITY
AHMEDABAD-382481
MAY-2017

Buckling behaviour of single-walled nanotubes

Major Project Report

submitted in partial fulfillment of the requirements

For the Degree of

Master of Technology in Mechanical Engineering

(CAD/CAM)

By

Ghata P.Tiwari

(15MMCC05)

Guided By

Dr. M.B Panchal



DEPARTMENT OF MECHANICAL ENGINEERING
INSTITUTE OF TECHNOLOGY
NIRMA UNIVERSITY
AHMEDABAD-382481
MAY-2017

Declaration

This is to certify that

- The thesis comprises my original work towards the degree of Master of Technology in Mechanical Engineering (CAD/CAM) at Nirma University and has not been submitted elsewhere for a degree.
- Due acknowledgment has been made in the text to all other material used.

Ghata P.Tiwari

(15MMCC05)

Undertaking for Originality of the Work

I, Ghata Tiwari, Roll No.15MMCC05, give undertaking that the Major Project entitled “Buckling behaviour of single-walled nanotubes ” submitted by me, towards the partial fulfillment of the requirements for the degree of Master of Technology in Mechanical Engineering (CAD/CAM) of Nirma University, Ahmedabad, is the original work carried out by me and I give assurance that no attempt of plagiarism has been made. I understand that in the event of any similarity found subsequently with any published work or any dissertation work elsewhere; it will result in severe disciplinary action.

Signature of Student

Date: -----

Place: Nirma University,Ahmedabad

Endorsed By

(Signature of Institute Guide)

Certificate

This is to certify that the Major Project entitled “Buckling behaviour of single-walled nanotubes ” submitted by Ms. Ghata P. Tiwari (Roll No: 15MMCC05), towards the partial fulfillment of the requirement for the degree of Master of Technology in Mechanical Engineering (CAD/CAM) of Institute of Nirma university, Ahmedabad is the record of work carried out by her under my supervision and guidance. In my opinion, the submitted work has reached a level required for being accepted for examination. The result embodied in this major project, to the best of my knowledge, haven't been submitted to any other university or institution for award of any degree or diploma.

Dr . M.B Panchal
Associate Professor,
Department of Mechanical Engineering,
Institute of Technology,
Ahmedabad.

Dr R N Patel
Professor and Head,
Department of Mechanical Engineering,
Institute of Technology,
Nirma University, Ahmedabad

Dr. Alka Mahajan
Director,
Institute of Technology,
Nirma University, Ahmedabad

Acknowledgments

With great pleasure I wish to express my deep gratitude to my project guide Dr. M.B.Panchal for his keen interest, constant encouragement and valuable guidance at all stages of this dissertation work. I am very much indebted to **Dr. R N Patel**, Professor and Head of Department of Mechanical Engineering, Institute of Technology, Nirma University, Ahmedabad for his valuable support, guidance and constant encouragement throughout my study. I am thankful to the faculty members of Mechanical Engineering Department, Institute of Technology, Nirma University, Ahmedabad for his help and inspiration in carrying out project. I am very much thankful to **Dr. Alka Mahajan** (Director, IT, NU) who have directly or indirectly helped me during this dissertation work. I would like to thank God Almighty, my parents and friends for their love, support and excellent co-operation to build my moral during the work.

Finally, I am thankful to all the faculty members of Mechanical Engineering Department, Laboratory assistants, Library staff and all my friends, colleagues who have directly or indirectly helped me during this project work.

Ghata P. Tiwari

Abstract

The non-linear mechanical response of the carbon nanotube, is said to be as their “buckling” behaviour, It is a major topic in the nanotube research community. Buckling is a deformation process in which a large strain beyond a threshold causes an abrupt change in the strain energy vs deformation profile. In the present work the single walled carbon nanotubes with different chirality, diameter and aspect ratio has been compared with single walled Boron Nitride nanotubes for critical compressive buckling forces analytically. Which resulted that with increase in nanotube aspect ratio, critical compressive buckling forces were decreasing and with diameter variation critical compressive forces were increasing. Furthermore, analysis of single walled carbon nanotube and single walled boron nitride with varying boundary condition, chirality, diameter, length and aspect ratio has been done for their critical buckling load trend and critical bending buckling strain, which resulted into decreased buckling load trends and buckling strains with increasing aspect ratios and increasing length. And also cylindrical shell theory FSDST was examined for buckling strains for armchair and zigzag configurations Hence, results were found to be consistent with simulated ones and suggested that buckling loads were reduced due to the transformations of NTs from shell buckling behaviour at small aspect ratios to beam buckling behaviour at larger aspect ratios. And buckling strains are not only found to be dependent on constrained boundary condition but also on the tube chirality and tube diameter. Therefore, when NTs are chosen as compression members their geometrical, material parameters and boundary conditions greatly affects the buckling forces and buckling strains

Contents

Declaration	iii
Certificate	v
Acknowledgments	vi
Abstract	vii
Table of Contents	ix
List of Figures	xii
List of Tables	xiv
Nomenclature	xv
1 Introduction	1
1.1 Nanotubes	1
1.1.1 Carbon Nanotubes	1
1.1.2 Boron Nitride Nanotubes	2
1.2 Types Of Carbon Nanotubes And Their Related Structures	3
1.3 Properties Of Nanotubes	4
1.4 Modeling Approach	4
1.4.1 Molecular Dynamics	5
1.4.2 Continuum Mechanics	5
2 Literature Review	6

3	Modelling for buckling analysis	13
3.1	Methodology	13
3.1.1	Euler's beam buckling load	14
3.2	Nonlocal Timoshenko beam equations and boundary conditions for buckling behavior of tubes	15
3.2.1	Load calculation	19
3.3	Shell theory	20
4	Results And Discussion	24
4.1	Analytical Results	24
4.1.1	Nanotube under compression	25
4.2	Non-local timoshenko beam equations	29
4.3	Nanotubes with different boundary conditions	32
4.3.1	CNT	32
4.3.2	BNNT	37
4.4	critical bending buckling strain	40
4.5	Examination of shell theory	41
4.6	Nanotubes with different boundary conditions using FSDST	46
4.7	CNT and BNNT Non-linear response	50
5	Conclusions and future scope of work	57
5.1	conclusion	57
5.2	Future Scope	58
	Bibliography	59

List of Figures

1.1	A carbon naotube	2
1.2	A boron nitride nanotube	3
1.3	Single double and Multi-Walled carbon naotube	4
3.1	Figure depicting rolling of Rolling of Hexagone sheet in two translational directions and different confugurations according to angle variations . . .	14
3.2	Single walled nanotube modeled as a beam or cylindrical shell	21
4.1	Comparison of armchair (3, 3) CNT and BNNT for the effect of nanotube aspect ratio on critical compressive buckling force	26
4.2	Comparison of zigzag (5, 0) CNT and BNNT for the effect of nanotube aspect ratio on critical compressive buckling force	27
4.3	Comparison of armchair (3, 3) CNT and BNNT for the effect of nanotube diameter on critical compressive buckling force	28
4.4	Effect of increasing nanotube aspect ratio on critical buckling forces $P_{cr}(nN)$ for the clamped-pinned rod based on nonlocal Timoshenko beam model .	30
4.5	Effect of increasing nanotube aspect ratio on critical buckling forces $P_{cr}(nN)$ for the clamped-pinned rod based on on local Timoshenko beam model . .	31
4.6	Effect of nanotube aspect ratio on critical compressive buckling force and critical buckling strain for clamped ends (armchair CNTs)	33
4.7	Deformed configurations of (8,8) CNT with deformations 1.23nm, 1.06nm , 1.02nm , 1.0nm after eigen buckling of lengths $l = 15, 20, 25, 30nm$ of clamped-ends	33
4.8	Effect of nanotube aspect ratio on critical compressive buckling force and critical buckling strain for pinned ends (armchair CNTs)	34
4.9	Deformed configurations of (8,8) CNT with deformations 1.00nm, 1.01nm , 1.00nm , 1.00nm after eigen buckling of lengths $l = 15, 20, 25, 30nm$ of pinned-ends	35

4.10	Effect of nanotube aspect ratio on critical compressive buckling force and critical buckling strain for clamped-free ends (armchair CNTs)	36
4.11	Deformed configurations of (8,8) CNT with deformations 1.00nm, 1.01nm , 1.00nm , 1.13nm after eigen buckling of lengths $l = 15, 20, 25, 30nm$ of clamped-free ends	36
4.12	Effect of nanotube aspect ratio on critical compressive buckling force and critical buckling strain for clamped ends (armchair BNNTs)	37
4.13	Effect of nanotube aspect ratio on critical compressive buckling force and critical buckling strain for pinned ends (armchair BNNTs)	38
4.14	Effect of nanotube aspect ratio on critical compressive buckling force and critical buckling strain for clamped-free ends (armchair BNNTs)	39
4.15	Comparison of simulated and analytical buckling strains of armchair configurations CNT for the effect of nanotube diameter	40
4.16	Comparison of simulated and analytical buckling strains of armchair configurations BNNT for the effect of nanotube diameter	41
4.17	Clamped-ends boundary condition for (12,0)	42
4.18	mesh design for cylindrical shell (at least 30 elements along circumferential length)	43
4.19	Comparison of critical buckling strains for various aspect ratios	44
4.20	Buckling modes of zigzag CNT (12,0) with different aspect ratios $l/d = 2.63, 3.48, 7.75, 16.27, 31.20$ using FSDST	45
4.21	Effect of nanotube aspect ratio on critical buckling strain of (5,5) for different boundary conditions	46
4.22	Buckling modes of (7,7) CNT for aspect ratios 3.01, 4.32 , 5.63 , 6.93 , 8.24 , 9.55 of clamped boundary condition	47
4.23	Buckling modes of (7,7) CNT for aspect ratios 3.01, 4.32 , 5.63 , 6.93 , 8.24 of clamped-free boundary condition	48
4.24	Effect of nanotube aspect ratio on critical buckling strain of (7,7) for different boundary conditions	48
4.25	Effect of nanotube aspect ratio on critical buckling strain of (10,10) for different boundary conditions	49
4.26	Effect of nanotube aspect ratio on critical buckling strain of (12,12) for different boundary conditions	50
4.27	Stresses and strains for (8,8) CNT for clamped-ends	51

4.28	Buckled geometrical configuration of (8,8) CNT	51
4.29	Strain energy v/s deformation profile for (8,8) CNT	52
4.30	Stresses and strains for (8,8) CNT for clamped-ends	52
4.31	Buckled geometrical configuration of (8,8) BNNT	53
4.32	Strain energy v/s deformation profile for (8,8) BNNT	53
4.33	A (13,0) CNT model	54
4.34	Eigen buckled deformation of (13,0) CNT	54
4.35	Buckled mode shape of CNT under compressive axial load	55
4.36	Buckled geometrical deformations after FEM eigen buckling analysis of (13,0) CNT	56

List of Tables

4.1	Aspect ratios and critical buckling forces for Armchair (3,3) CNT	25
4.2	Aspect ratios and critical buckling forces for Armchair(3,3) BNNT	25
4.3	Aspect ratios and critical buckling forces for Zigzag(5,0) CNT	26
4.4	Aspect ratios and critical buckling forces for Zigzag(5,0) BNNT	26
4.5	Effect of variation in diameter on critical compressive force for armchair CNT	27
4.6	Effect of variation in diameter on critical compressive force for armchair BNNT	27
4.7	Local buckling eular load(Pe) , Non-local timoshenko and Local timo- shenkobuckling force $P_{cr}(nN)$ for the clamped-pinned rod for $e_0a = 0$. . .	29
4.8	Local buckling eular load(Pe) , Non-local timoshenko and Local timo- shenkobuckling forces $P_{cr}(nN)$ for the clamped-pinned rod for $e_0a = 0.5$. .	30
4.9	Local buckling eular load(Pe) , Non-local timoshenko and Local timoshenko buckling forces $P_{cr}(nN)$ for the clamped-pinned rod for $e_0a = 2$	30
4.10	Geometrical parameters and buckling forces for clamped CNTs	32
4.11	Geometrical parameters and buckling forces for Pinned CNTs	34
4.12	Geometrical parameters and buckling forces for clamped-free CNTs	35
4.13	Geometrical parameters and buckling forces for clamped end BNNTs	37
4.14	Geometrical parameters and buckling forces for pinned end BNNTs	38
4.15	Geometrical parameters and buckling forces for clamped-free BNNTs	39
4.16	Geometrical parameters and crititcal strain value for armchair CNT	40
4.17	Geometrical parameters and crititcal strain value for armchair BNNT	41
4.18	Critical buckling strains for armchair and zigzag configurations	43
4.19	Crititcal buckling strains for different boundary condition for armchair (5,5) configuration	46

4.20	Critical buckling strains for different boundary condition for armchair (7,7) configuration	47
4.21	Critical buckling strains for different boundary condition for armchair (10,10) configuration	49
4.22	Critical buckling strains for different boundary condition for armchair (12,12) configuration	49
4.23	Stresses and strains for different lengths of (8,8) for clamped CNT	50
4.24	Stresses and strains for different lengths of (8,8) for clamped BNNT	52
4.25	Geometrical parameters and deformations after non-linear response	55

Nomenclature

variables	Physical Quantity
E	elastic modulus
μ	poisson' ratios
θ	angle
h	thickness
G	shear modulus
l	length
d_o, d_i	outer diameter and inner diameter
K	effective length of the coumn
a	bond length of between c-c
ε_{cr}	critical srain
F_{cr}	critical compressive force
C_h	chiral vector
r	tube radius

Chapter 1

Introduction

1.1 Nanotubes

Nanotubes are very small in size and are measured in nanoscale . They are found in the form of Single Walled and Muti Walled Nanotube. Nanotubes belongs to the fullerene structural family . Both Carbon and Boron Nitride nanotubes are capable of resisting high strain without breaking.

.

1.1.1 Carbon Nanotubes

Carbon Nanotubes (CNTs) were discovered by lijima[1] . They are allotropes of carbon with a cylindrical nanostructure . These cylindrical carbon molecules have different properties , these finds applications in electronics, optics and other fields . They possess extraordinary material strength and stiffness, Significantly larger than for any other material . Their long and hollow structure with the walls formed by one-atom-thick sheets of carbon called graphene .

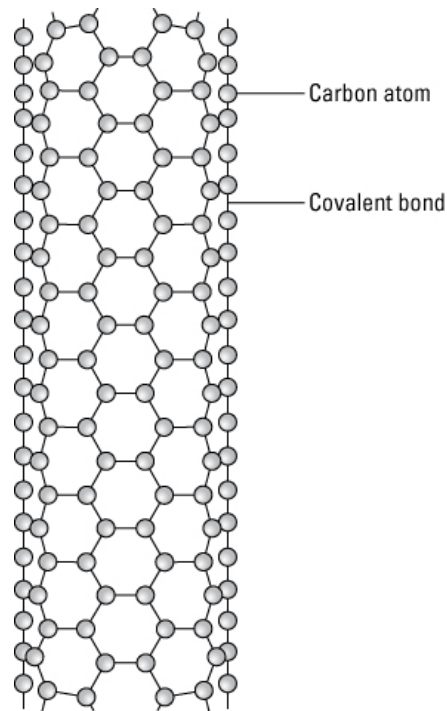


Figure 1.1: A carbon naotube

1.1.2 Boron Nitride Nanotubes

Boron Nitride Nanotubes (BNNTs) are polymorph of boron nitride . BNNTs were predicted in way back to 1994[2] and experimentally successful discovered in 1995[3]. On structural basis they are similar to the carbon nanotube , Here in there takes a substitution of carbon atoms by nitrogen and boron atoms. However, the properties of boron nitride nanotubes differs .Carbon nanotubes can behave as a metallic or semiconducting depending on their wrapping direction and radius , A BN nanotube is an electrical insulator with a bandgap of $\approx 5.5\text{eV}$. Further, a layered BN structure is very much stable in their thermal and chemical states than a graphitic carbon tubular structure

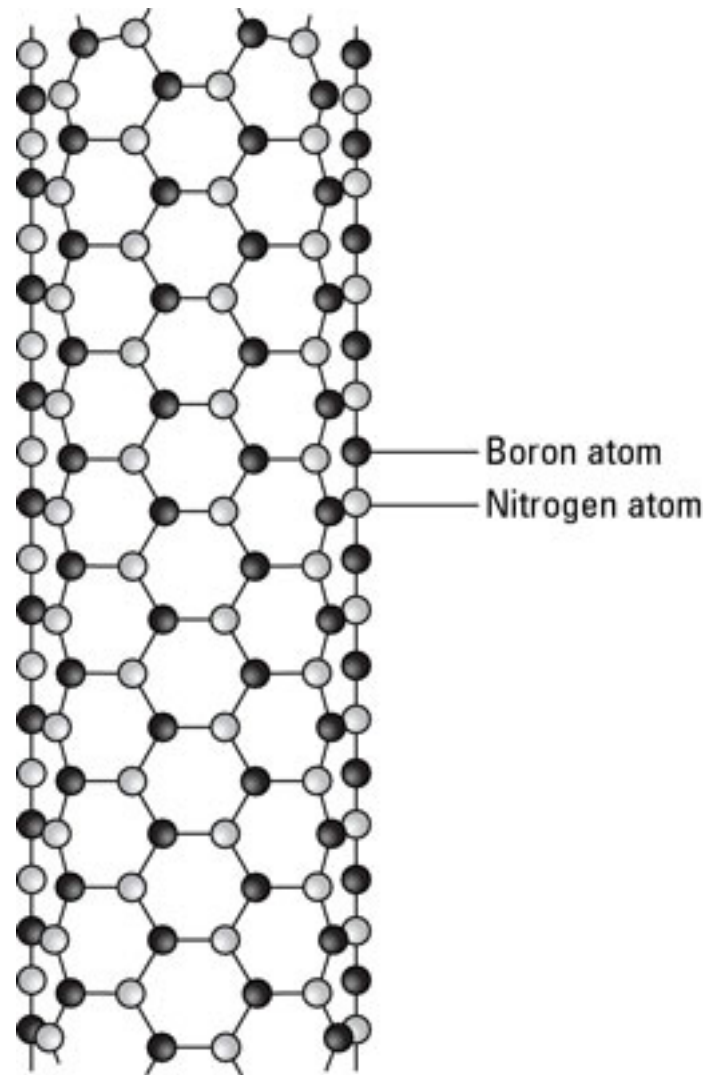


Figure 1.2: A boron nitride nanotube

1.2 Types Of Carbon Nanotubes And Their Related Structures

1. Single Walled Carbon Nanotube

single-walled Nanotubes (SWNTs) have diameter of about 1 nanometer , and upto millions of times longer . The structure of SWNT can be conceptualized by curling of a one-atom-thick layer of graphitic sheet called graphene into seamless cylinder . The way the graphene sheet is curled is represented in the form of indices named (n,m) . Integers n and m represents the number of unit vectors along the two directions in the Honeycomb crystal lattice or hexagone graphene . If $m=0$ the nanotubes are called Zigzag Nanotubes and if $n=m$, the nanotubes are called Armchair Nanotubes . Otherwise they are called chiral . The diameter of an ideal nanotube can be calculated from its (n,m) indices as follows :

$$d = \frac{a}{\pi} \sqrt{n^2 + nm + m^2} = 78.3 \sqrt{((n+m)^2 - nm)} pm \quad (1.1)$$

Where $a = 0.246$ nm

2. Double-walled Nanotubes(DWNTs) Double walled nanotube forms a special class of nanotubes because of their morphology . And their properties are similar in comparison with SWNTs .

3. Multiwalled Nanotubes (MWNTs) Multiwalled nanotubes have multiple layers which are rolled at specific angles and resulting in vaying mechanical properties .

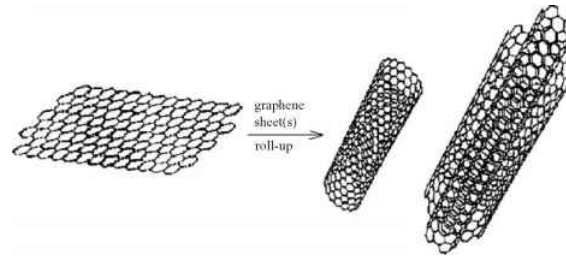


Figure 1.3: Single double and Multi-Walled carbon naotube

1.3 Properties Of Nanotubes

CNNT and BNNT possess extra ordinary mechanical properties with CNT 1TPa And for BNNT IS 1.24 TPa. Furthermore, the thermal properties of CNT is found to be around 6000W/mK . The BNNT have good thermal and oxidation stabilites than CNT. Through experimental investigations it was found that physical property such as conductance of CNTs are strongly influenced by the occurrence of buckling . Thus, the reversible transformation between the buckled state and normal state of CNTs leads to potential applications such as nanostrain sensors and actuators , nanofluidic components and carbon reinforced composites .

1.4 Modeling Approach

The experimental investigations of buckling behaviours of CNTs remains a challenge because of difficulties encountered at nano-scale and time length scales . The computational approach is better for CNT by providing simulation results to help the understanding , analysis and design of such CNT . There were two theoretical and numerical approaches to understand the buckling Behavior of CNTs :

1.4.1 Molecular Dynamics

With the developed accurate force field the molecular dynamics nowadays have been important and useful for the simulations of CNTs behaviors' at the nano-scale level . In molecular dynamics approach the atoms are considered as individual particles or points and the forces acting between each particle and other bonded particle is calculated using the potential theories . The dynamic equation for each atom is established for the determination of displacement fields under given loading conditions . The atomistic interactions in CNT and individual atom is being modeled by employing the force fields .

1.4.2 Continuum Mechanics

In this approach the CNTs are primarily modeled as a continuous beams or thin shells with a fixed effective wall thickness , young's modulus and Poisson's ratio . The buckling behavior of SWCNTs is investigated by using continuum shell model and beam model . When the aspect ratio between the length , l and diameter d is larger the mechanical behavior of SWCNTs approaches that of a beam .

Chapter 2

Literature Review

- Helical microtubules of graphitic carbon - Sumio Iijima [1]

fabrication of carbon in the molecular form and other structure generated interests for graphitic carbon sheets. Author inferred here about the carbon structure consists of tubes which are in the form of needle type. The process arc discharge of evaporation was found to have similarity with that used for synthesis of fullerenes. The needles were found to have grown on the cathode terminal. Process employed like electron microscopy resulted that needle is made up of graphite sheets which are in coaxial form. Graphite sheets were found to have range between 2 to 50. On every needle carbon atom hexagonal helical patterns were arranged about the tube axis. In the single needle helical pitch was varying from one tube to other. This suggested that helical pattern can be very helpful in growth process. Diameters for needle were ranging from few to few nanometers.

- A review on the application of nonlocal elastic models in modeling of carbon Nanotubes and graphenes - B. Arash, Q. Wang [4]

Carbon nanotubes from graphene sheet can be modelled with the employment of nonlocal continuum theory. Nonlocal continuum model varies for the materials under the static and dynamic conditions. For the nonlocal continuum models it is necessary to incorporate small scale parameter and it was found to give better results. Moreover, there are chances of complicated equations if higher order continuum models are employed. For CNTs with small aspect ratio elastic shell models form the basis of modelling and static and dynamic conditions. And for long CNTs nonlocal Euler-Bernoulli beam models were used.

- Theory of growth and mechanical properties of nanotubes - J. Bernholc, C. Brabec, M. Buongiorno Nardelli, A. Maiti, C. Roland, B. I. Yakabson [5]

In this part the author reviews about the kinetics behind the deformation of carbon due to the strain under tensile conditions which are on long time scale for their simulation in classic molecular dynamics on long CNTs. Because of this reason the author carried out his study on the time scale transitions for long CNTs. Under axial strain of 10% system was found to be evolved at about 2.5ns, with increased rate of temperature at 5050k/ps after the initial annealing process is done on 2000k. Hence, when there are large deformations for the mechanical properties structural changes are rapid and switching into varied morphological trends.

- Bending and buckling of carbon nanotubes under large strain – M.R.Falvo, G.J Glary, R.M Taylor, F P Brooks, Jr. S. Washburn & Superfine [6]

When graphite sheet is being wrapped results with certain rolling energy and vector indices results into carbon nanotubes which were found to have excellent mechanical and electrical properties. They were found to have high modulus of elasticity which influenced that they might be stiffer and stronger in comparison with other material. Because of this they are found to have their wide applications in nanocomposites and sensor sthata at nanometerd scales. These nanotubes can also have defects which suggest that individual nanotubes should be considered with proper measurements so that they results in nanotubes with good mechanical properties.

- Collapse of Single walled carbon nanotube is diameter dependent – James A. Elliot Jan K.W Sandler, Alan H Windle, Robert J. Young AND Milo S. P. Shaffer [7]

Author did series of analysis on carbon naotubes under hydrostatic pressure for validating hypothesis that forms the basis that they undergo variable changes. Here, he reviewed that analysis which were being carried out and were in accordance with the hypothesis and was found that chirality was not much significant, diameter was found to be of much importance to get the pressure values. Diameter was also found to be as limitation if they were large or depicting the behaviour of SWCNT related with their stabilities. Through simulations author predicted critical diameter to be 4.2 and 6.9nm at atmospheric pressure.

- Effects of chirality and boundary conditions on mechanical properties of Single walled carbon nanotubes- Guoxin Cao and Xi chen [8]

When bending load is applied on CNT it is found to be very sensitive for chirality and the boundary conditions applied. Deformed pattern was found to be same for nanotube if it is axially compressed. If the rotating boundary condition is applied the tube gets easily buckled, but the ε_{cr} bending difference between armchair and zigzag was found to

be small and it was reported about 15%. But the rotating boundary conditions tends to reduce the tube due to strain produced in tube. Due to the ε_{cr} bending ends of tubes were stress concentrated and this steadily leads to the small snap buckling. It was also reported that ε_{cr} compression was about 20% than the counterparts which were not in the constrained condition But were in bending and with further increase in circular boundary conditions the snap buckling was shifted in the middle of the nanotube.

- Mechanics of deformation of SWCNT and MWCNT - Antonio pantano , David M.Parks , Mary C. Boyce [9]

Author reviews about the need of a lattice shifting from a plane hexagon pattern which is not under any stress condition to form a wrapped carbon tubule which is having some stress concentrations due to their changed curvature of geometry from sheet to tube. For modelling of nanotubes FE codes were used which accounts for pre-existing stress state. Secondly, the inner wall-wall interactions within the nanotube structure. It was found by analysis & theoretical studies that shear resistance was very less. So, it can be taken as zero for approximating the model.

- Nanomechanics of carbon nanotubes : instabilities beyond Linear Response – B.I.Yakobson , C.J Brabec and B. Bernholc [10]

CNTs sustain extreme strain conditions with no brittle fracture and complete deformations, or any transitions at atomistic levels. Their non-linear behaviour of continuum means beyond hook's law can be well approximated by considering the elastic parameters. When the deformations are very large there is a sudden strain energy release which resulted into geometry reversibilities and different morphological trends. Estimation with effective elastic parameters of the continuum model for buckling can be done by using the equation given in paper by author which were in accordance with simulation results.

- Prediction of Buckling characteristics of Nanotubes – N.Hu , K Nunoya , D.Pan , T .Okabe, H.Furukunga [11]

The author briefs about the effective approach, i.e. MSMA, for the Buckling analysis of carbon nanotubes. A beam is employed by the author for modelling C-C covalent bonds in nanotubes. Furthermore a beam element is used for modeling carbon atoms between two different walls by van der Waals force. When CNT is capped the transitions were not much to predict buckling behaviours because beam buckling was happening, When both ends of CNT were pinned the effect was not of much importance. However, when the CNT was fixed - free and capped it was found that it aided the shell buckling load about 50%. Capped CNT was found to act as more effective way by changing boundary constraints from free-fixed to pin-fixed.

- A structural mechanics approach for the analysis of carbon nanotubes – Chunyu Li and Tsu -Wei Chou [12]

By employing effective MSMA approach for the prediction of buckling of CNT , the C-C atom acted as load carrying members and C atoms as joints for the load carrying members . By bridging molecular structural mechanics approach and molecular mechanics approach CNT can be modelled as a beam or shell . It was gleaned that Young's moduli is greatly affected by doing variations in nanotube diameter and helical pattern. With increase in nanotube diameter it was found that armchair and zigzag predicted young's moduli to that of graphite.

- Thickness of graphene and Single Walled Carbon Nanotubes – Y . Huang , J Wu And K.C Hwang [13]

From the theories of potential which were obtained from interatomic potential can be used to determine elastic modulus and thickness of CNTs. The thickness of CNT was found have dependence on the boundary constraints such as (uniaxial tension, equibiaxial stretching, uniaxial stretching) and the radius of nanotube ($R < 1\text{nm}$) . So, from atomistic simulations thickness can be computed . Hence , the approach used here can be used to stress free state of CNT and multiwall CNT which were found to be very complex for the simple constraints such as uniaxial tension due to van der Waals' interaction between multiwalls of CNT .

- Structural flexibility of carbon nanotubes – Sumio Iijima , Charles Brabec , Amitesh maiti and Jerzy Bernholc [14]

Under combined mechanical loading conditions bending and buckling of single and multi walled carbon nanotubes was reported by author with high resolution images and atomistic simulations . With the increase in bending angles single and multiple snap buckles were found to be reported , and occurring of kinks explained by atomistic simulations because they employ real body potentials . Author results suggests that if bending angle is increased , the structures can be fully reversed in spite of the presence of high strains on the ends of the tube and multiple snap buckles. These possibilities are due to honeycomb structure , which was found to be very flexible in nature , and resisted bond stretching and inversion under the high strained tube regions and vice-versa.

- Buckling of Single-walled carbon nanotubes upon bending: Molecular dynamics simulation and finite element method – Guoxin Cao and Xi Chen [15]

Author reports that there is not length dependence for continuum model for their bending buckling curvature . Whereas from MD analysis author reports that if aspect ratio is beyond

or less than the threshold value of aspect ratio the critical bending buckling curvature was found to be decreasing. Values of the (l/D) threshold and the critical bending buckling curvature goes on decreasing with increase in radius for the tubes. After buckling results from molecular dynamics gave inference that the deformed geometries are directly in relation with threshold aspect ratio value. If the values of aspect ratio is less than threshold the single kink is formed at the middle of the tube if greater than threshold kink is formed at ends of the nanotubes.

- Continuum shell model for buckling of Single walled carbon nanotube with different chiral angles - Amar Nath Ray Chowdhury, Chien ming Wang and Soo Jin Adrian Koh [16]

When the chirality is varied the critical buckling load/strain value was found to vary from series of MD simulation was found. The value for critical buckling load/strain value from zigzag was found to be higher than that of armchair with chiral angle of θ^0 and the chiral angle $\theta=20^0$ had the lowest value for critical buckling load/strain. An empirical relationship for elastic moduli which is dependent on the diameter d and θ is obtained. By using $\nu=0.19$ and $h=0.066\text{nm}$, the continuum model is able to predict critical buckling load/strain values for close approximations.

- Bending buckling behavior of Single and multi walled carbon nanotubes – Xiaohu Yu, Qiang Han, Hao Xin [17]

The different SWCNTs with chirality and length, the critical bending buckling curvature reduces steeply because as it is the inverse square of the tubule diameter and here the chirality of nanotube is found to be insignificant. Author gave conclusions that are in agreement with results of MD and published papers of Cao and Chen, Lijima, Yakobson. Inter layer van der Waals force in MWCNTs greatly affects the bending buckling curvature, loads and after buckling results.

- Atomistic simulations of nanotube fracture – T. Belytchko, S.P Xiao, G.C Schatz And R.S Ruoff [18]

Under molecular mechanics simulations nanotube fracture was found and its dependence was not on separation energy from body potentials but was dependent on interatomic potentials. When experimentally compared the nanotube fracture of zigzag was found to be in between 10-15%. Stress fracture range predicted by author was 62-93 GPa. By computational methods fracture for armchair and zigzag was found to be higher. Differences in values of small scale defects for failure stresses are in agreement with already available simulation results. From atomistic simulations brittle fracture and strain can be obtained.

- Modeling of single walled carbon nanotube by molecular structural mechanics approach - Chunyu Li , Tsu Wei Chou [19]

This paper gave insight of about the elastic buckling of carbon nanotubes by applying the Molecular structural mechanics method. The effects of nanotube diameter , aspect ratio and tube chirality on critical force is being found out. Critical compressive buckling force is higher than bending buckling force , With successive increase in (L/d) the critical compressive and bending force decreases . The variations in trends of critical buckling load when plotted with nanotube diameter was found to be similar for SWCNTs and DWCNTs.

- Effective structural parameters of single walled carbon nanotubes – K.Yazdchi , M. Salehi and M.M Shokreh [20]

Author reviews that CNT buckling behaviour can be predicted by continuum model by employing force potentials , UFF and molecular mechanics approach . The CNT can be thought of it by assumption that it act as a space frame structures when carbon atoms start acting as a load bearere .On the basis that beams are used and trusses in the form of truss. Length , chirality and diameter can be found out . With increase of tube diameter , elastic modulus and shear modulus for armchair CNT and zigzag CNT resulting in increase of elastic parameters of graphene sheet , hence varying pattern is reversible for poisson's ratio . and effectively wall thickness and Vdw on behavior of SWCNT.

- Deformation Mechanisms of very long Single- walled carbon nanotubes subjected to Compressive loading – Markus J. Buehler , Yong Kong , Huajian Gao [21]

Author describes about that SWNTs when they are compressed axially their resulting deformations which are different according to the process as the (L/d) ratio is increased . Outputs, suggest that are three different classes for nanotubes of their resulting deformations when they are under compressed loading condition like nanotubes which are having small (l/d) ratio . The deformed geometrical patterns is due to their cylindrical shell tubule .Above the limits for (l/d) for buckling of shell switches into the beam buckling mode . Changing from shell buckling to beam buckling analysis values for critical (l/d) is $(\mu_r \approx 12.5)$. And for large (L/d) SWCNTs are found to be deformed into the helix structures that . when the (l/d) is much more larger then their deformation results leads them to behave like a biomolecule. From this it is observed that the behavioral geometrical mechanical deformations changing from shell -to -beam and beam -to- shell is due to increasing (l/d) ratios.

- Prediction of stiffness and strength of single-Walled carbon nanotubes by molecular Mechanics approach based finite element approach – Xuekun Sun , Wenming Zhao [22]

Author findings predict that stiffened property of CNT is not much dependent on the diameter of tube and its helix structure, but Poisson's ratio is found to be dependent on nanotube diameter. To model the bondbreaking of C-C modified Morse potential function was used with 7.7eV separation energy. Fracture strain was found to be around 0.3 with strength in between the 77-101GPa of CNT. Nanotube helix structure was observed to be independent of diameter of nanotube, but was dependent on nanotube diameter. With successive increment of nanotube diameter caused reduction in Poisson's ratio which was in the range of 0.1-0.35.

- Finite element modeling of SWCNT - K.I Tserpes, P. Papanikos [23]

Author proposed the model developed which was having influence on length and chirality on critical loads. Author assumed that when SWCNTs are loaded they start behaving like space members with carbon atoms bond acted as load bearer. As FE model of CNT can be done by nodes placement on the place of carbon atom and c-c bonding by three-dimensional rod or beam elements. Bridging of molecular mechanics and structural mechanics was used to obtain Young's moduli between beam elements. For evaluation purpose and performance of CNTs tube wall thickness was found to be of much greater importance because it also helped in the determination of the effect of nanotube diameter, wall thickness and chirality on Young's modulus.

- Elastic properties of Boron nitride nanotubes and their comparison with carbon Nanotubes - Mogurampelly Santosh, Prabal K maiti and A .K Sood [24]

Author summarizes that boron nitride nanotubes (BNNTs) are having boron nitrogen atom in honeycomb structure because of larger charges on the boron and the nitrogen atoms. Therefore, there electrostatic interactions might help in determining the effective elastic parameters. In the absence of their unique partial atomic charge information for the boron and nitrogen the Young's and the shear modulus of BNNT function as of the tube radius and the number of walls uses molecular mechanics analytical calculation. The strain energy is in direct proportion to $1/R^2$ for BNNTs and CNTs. Calculations show that Young's modulus for BNNT is 1.04TPa having $\pm 0e$ and $\pm 0.41e$ charge on B/N atoms, 1.14 TPa with $\pm 0.68e$ on B/N Atoms, 1.22 TPa with $\pm 1.0e$ charge on B/N atoms and 1.38 TPa with $\pm 1.41e$ charge on B/N atoms for larger radius of tube and of the CNT is 1.07 TPa. Young's modulus of BNNT is more than that for CNT of $\pm 0.68e$, $\pm 1.0e$ and $\pm 1.41e$ charge on B/N atom.

Chapter 3

Modelling for buckling analysis

On Macrolevel, a nanotube can be prepared by modelling it as a cylinder continuum having transversely isotropic mechanical properties . Various , kinds of atomistic finite elements such as rods, trusses , beams and springs are used to model C-C covalent bonds in CNTs [25] . Giannopoulos et.al [26] proposed computaional finite element model for simulating the SWCNT for lineared interatomic potential .

On macroscale, a model which considers the continuum modelling approach which in conjunction takes effective young's modulus and effective parameters such as poisson's ratio , wall thickness from a molecular mechanics approach . computationally this approach is best suited for the modelling of SWCNT with proper outcomes for simulation results with different chiralities and effective parameters .

3.1 Methodology

A nanotube can be modeled by rolling a graphene sheet in two directions . Two chiral indices (n,m) which defines the cylindrical configuraton as it on a CNT . n is usually greater than . where (n,n) can be named as armchair and (n,0) as zigzag. The tranlational vector T , which is paralleled to the main tube axis and is being perpendicular to the chiral vector C_h . Unit vectors of the grahene sheet are lying along two zig-zag lines , and is represented as a_1 and a_2 . Vector a_1 and a_2 have diiferent magitudes and if they are added it comes out to be equal chiral vector C_h [27]. The formula given below is used to compute the value of diameter of nanotube d_{NT} for different configurations.

$$d_{NT} = \frac{a_{c-c}\sqrt{3(n^2 + nm + m^2)}}{\pi} \quad (3.1)$$

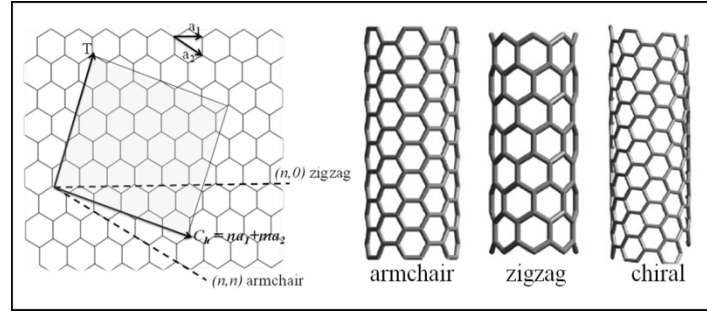


Figure 3.1: Figure depicting rolling of Rolling of Hexagone sheet in two translational directions and different configurations according to angle variations

[28][29][30]

3.1.1 Euler's beam buckling load

The experimental investigation of buckling behavior remains a challenge because of difficulties encountered at the Nano-scale. Therefore, The computational approach is better by providing simulation results to help the understanding, analysis and design of such Nanotube. And the theoretical and numerical approaches were molecular dynamics and continuum mechanics.

From the viewpoint of molecular mechanics, a nanotube can be regarded as a large molecule consisting of carbon or boron atoms. The atomic nuclei can be regarded as material points. Their motions are regulated by a force field, which is generated by electron–nucleus interactions and nucleus–nucleus interactions Machida, 1999 [21]. Usually, the force field is expressed in the form of steric potential energy. It depends solely on the relative positions of the nuclei constituting the molecule.

And by continuum mechanics meaning the Cylindrical shell can be approximated by considering appropriate wall thickness, elastic modulus and poisson's ratio Dresselhaus et al., 1995[22], the critical loading is calculated according to the classical Euler formula for columns Chen and Lui, 1987[23] here, [11]

$$CriticalCompressiveBucklingForce (nN) (Fcr) = \frac{\pi^2 EI}{Kl^2} \quad (3.2)$$

For rods/tubes with pinned ends, $K = 1$

For rods/tubes with clamped ends, $K = 4$

For rods/tubes with clamped-free ends, $K = 2$

K = Effective length of column,

Fcr = Critical compressive force (nN)

And, moment of inertia is,

$$\text{MomentOf inertia}(I) = \frac{\pi(d_o^4 - d_i^4)}{64} \quad (3.3)$$

Whereas , d_o = outer diameter of nanotubes d_i = inner diameter of nanotubes

Here, Where E is the Young's modulus of the carbon Nanotube in (Tpa), I is the cross-sectional Inertia about one of .its symmetric axes and l is the nanotube length.

3.2 Nonlocal Timoshenko beam equations and boundary conditions for buckling behavior of tubes

To capture the small scale effect in mechanical properties for nanotubes the non local timoshenko beam thory and equations are used by researchers for the buckling analysis of nanotubes for their potential applications . For the present work the small scale effect using timoshenko beam load equations for clamped boundary condition for the computation of critical buckling force has been done numerically .

According to timoshenko beam theory strain-displacement is given by:[31]

$$\varepsilon_{xx} = z \frac{d\Phi}{dx}, \quad (3.4)$$

$$\gamma_{xz} = \Phi + \frac{dw}{dx} \quad (3.5)$$

x is longitudinal , z coordinate from neutral axis of beam , w transverse displacement , Φ rotation due to bending , ε_{xx} normal strain and γ_{xz} transverse shear strain

The virtual strain energy δU is given by

$$\delta U =_0 \int \int_A (\tau_{xx} \delta \varepsilon_{xx} + \tau_{xz} \delta \gamma_x) dA dx, \quad (3.6)$$

where, τ_{xx} is normal stress , τ_{xz} transverse shear stress , L length of the beam and A area of cross-section of beam .

on substitution of (3.5) and (3.6) virtual strain energy is expressed as ,

$$\delta U = \int_0^L (M \frac{d\delta\Phi}{dx} + Q(\delta\Phi + \frac{d\delta w}{dx})) dx \quad (3.7)$$

$$M = \int_A \tau_{xx} z dA \quad (3.8)$$

$$Q = K_S \int_A \tau_{xz} dA \quad (3.9)$$

M and Q are bending moment and shear force where K_s is shear correction factor of the timoshenko beam theory [11,12] which compensates for the error in assuming a constant shear strain (or stress) through the beam thickness.

Assuming that the rod/tube is subjected to an axial compressive load P the virtual potential energy δV , of the axial load is given by

$$\delta V = - \int_0^L p \frac{dw}{dx} \frac{d\delta w}{dx} dx \quad (3.10)$$

from principle of virtual displacements i.e, total virtual work done should vanish if a body is in equilibrium

$$\delta W = \delta U + \delta V \quad (3.11)$$

Thus from the equations (3.9) and (3.12), we have

$$\delta W = 0 = \int_0^L \left(M \frac{d\delta}{dx} + Q \left(\delta\Phi + \frac{d\delta w}{dx} \right) - p \frac{dw}{dx} \frac{d\delta w}{dx} \right) dx \quad (3.12)$$

By performing integration by parts, we obtain

$$0 = \int_0^L \left[\left(-\frac{dM}{dx} + Q \right) \delta\Phi + \left(-\frac{dQ}{dx} + P \frac{d^2 w}{dx^2} \right) \delta w \right] dx + [M] + \left[Q \delta\Phi - p \frac{dw}{dx} \right] \delta w \quad (3.13)$$

Since $\delta\Phi$ and δw are arbitrary in $0 < x < L$, therefore the obtained Resultant equilibrium equations are

$$\frac{dM}{dx} = Q \quad (3.14)$$

$$\frac{dQ}{dx} = P \frac{d^2 w}{dx^2} \quad (3.15)$$

Boundary Condition for beam theory is given by:

Specify

$$w \text{ or } Q - P \frac{dw}{dx} \quad (3.16)$$

specify

$$\phi \text{ or } M = 0 \quad (3.17)$$

The simplified non local constitutive equation for the local stress and strain in a one-dimensional case is given by:

$$\tau_{xx} - (e_0 a^2) \frac{d^2 \sigma_{xx}}{dx^2} = E \varepsilon_{xx} \quad (3.18)$$

Where τ_{xx} is the normal stress, ε_{xx} the normal strain, E the young's modulus and $e_0 a$ the scale coefficient that incorporates small scale effect . here, a is internal characteristic length (e.g. lattice parameter, c-c bond length) .The constitutive relation for the shear stress and strain remains the same as in local beam theory that is,

$$\tau_{xz} = G \gamma_{xz} \quad (3.19)$$

Where σ_{xz} is the transverse shear stress and γ_{xz} the transverse shear strain and G the shear modulus . No nonlocal effect is injected into the shear constitutive relation

Multiplying equation (20) by $z dA$ and integrating result over the area yields

$$M - (e_0 a) \frac{d^2 M}{dx^2} = EI \frac{d\phi}{dx} \quad (3.20)$$

Where I is the second moment of inertia . Also by integrating equation (3.21) over the area one obtains,

$$Q = K_s GA \left(\phi + \frac{dw}{dx} \right) \quad (3.21)$$

Where K_s is the shear correction factor

on substitution of equation (18) and (19) into (20) we get,

$$M = EI \frac{d\phi}{dx} + P (e_0 a) \frac{d^2 w}{dx^2} \quad (3.22)$$

When characteristic length is set to zero the equation (23) reduces to that of a local timoshenko model

From the view of equations (23) and (24) the governing equations for buckling of nonlocal timoshenko beams are given by

$$EI \frac{d^2 \omega}{dx^2} + (e_0 a)^2 P \frac{d^3 \omega}{dx^3} - K_s GA \left(\phi + \frac{dw}{dx} \right) = 0 \quad (3.23)$$

$$K_s GA \left(\frac{d\Phi}{dx} + \frac{d^2 w}{dx^2} \right) - P \frac{d^2 w}{dx^2} = 0 \quad (3.24)$$

Based on equations (18) and (19), the two boundary conditions associated with nonlocal timoshenko beam theory, at each end of the beam are given by:

$$w = 0., M = EI \frac{d\Phi}{dx} + P(e_0 a^2) \frac{d^2 w}{dx^2} = 0 \quad (3.25)$$

for a pinned end,

$$w = 0., \Phi = 0 \quad (3.26)$$

$$M = EI \frac{d\Phi}{dx} + P(e_0 a^2) \frac{d^2 w}{dx^2} = 0 \quad (3.27)$$

for a clamped end,

$$Q - P \frac{dw}{dx} = K_s \Phi + \frac{d\delta w}{dx} - P \frac{dw}{dx} = 0 \quad (3.28)$$

for a free end

3.2.1 Load calculation

Displacement and rotation equations for elastic buckling is given by:

$$\frac{d^4 \dot{w}}{dx^4} + K \frac{d^2 \dot{w}}{dx^2} = 0 \quad (3.29)$$

$$\frac{d^3 \dot{\Phi}}{dx^3} + K \frac{d \dot{\Phi}}{dx} = 0 \quad (3.30)$$

$$\dot{w} = w/l, \quad (3.31)$$

$$x' = x/landK = \frac{Pl^2/EI}{[1 - \frac{p}{k_s GA} - (e_0 a)^2 \frac{P}{EI}]} \quad (3.32)$$

General solution is given by [13]:

$$\dot{w} = C_1 \text{Sin} \sqrt{Kx'} + C_2 \text{Cos} \sqrt{Kx'} + C_3 x' + C_4 \quad (3.33)$$

$$\dot{\Phi} = -C_1 \sqrt{K} \left(1 - \frac{P}{k_s GA}\right) \text{Cos} \sqrt{Kx'} + C_2 \sqrt{K} \left(1 - \frac{P}{k_s GA}\right) \text{Sin} \sqrt{Kx'} - C_3 \quad (3.34)$$

Here C_1, C_2, C_3, C_4 , are unknown constants. From eigen value problem we got the equation for critical load

And critical load equations for different loading condition is given as below:

for pinned end ,

$$P_E = \pi^2 EI/l^2 \quad (3.35)$$

for clamped end

$$P_E = 4\pi^2 EI/l^2 \quad (3.36)$$

for free end

$$P_E = 4\pi^2 EI/(4l^2) \quad (3.37)$$

3.3 Shell theory

The Euler buckling load equations and non-local timoshenko beam equations mentioned above were used for the computation of compressive buckling forces for different configurations and boundary conditions which could be helpful in computation of mechanical properties of nanotubes . As like this the First order deformation shell theory(FSDST) cylindrical shell theory can be used for the predictions of critical buckling strains . FSDSTs governing equations are being mentioned overhere for single-walled carbon nanotube (CNTs).where, μ is poisson's ratio, h is the shell thickness and R shell radius , E is the young's modulus i.e.5.5Tpa, I is the second moment of inertia ; L is the length of CNT , K_s is the timoshenko shear correction factor=9/10 for a circular tubr , G is the shear modulus=450Gpa , A is the cross-sectional area of CNT and buckling factor K is $4\pi^2$ for clamped ends .

Consider a cylindrical shell having cylindrical coordinates as (x, θ, r) as shown in fig.The equilibrium equations of the cylindrical shell under the action of axial compressive load is given by :

$$\frac{\partial N_{xx}}{\partial x} + \frac{1}{R} \frac{\partial N_{x\theta}}{\partial \theta} - \frac{s_1}{2R} \frac{\partial M_{x\theta}}{\partial \theta} = 0 \quad (3.38)$$

$$\frac{\partial N_{x\theta}}{\partial x} + \frac{1}{R} \frac{\partial N_{\theta\theta}}{\partial \theta} + \frac{s_1}{2R} \frac{\partial M_{x\theta}}{\partial \theta} + s_2 \frac{Q_\theta}{R} = 0 \quad (3.39)$$

$$\frac{\partial Q_x}{\partial x} + \frac{1}{R} \frac{\partial Q_\theta}{\partial \theta} - \frac{N_{\theta\theta}}{R} - N \frac{\partial^2 c}{\partial x^2} = 0 \quad (3.40)$$

$$\frac{\partial M_{xx}}{\partial x} + \frac{1}{R} \frac{\partial M_{x\theta}}{\partial \theta} - Q_x = 0 \quad (3.41)$$

$$\frac{\partial M_{xx}}{\partial x} + \frac{1}{R} \frac{\partial M_{\theta\theta}}{\partial \theta} - Q_\theta = 0 \quad (3.42)$$

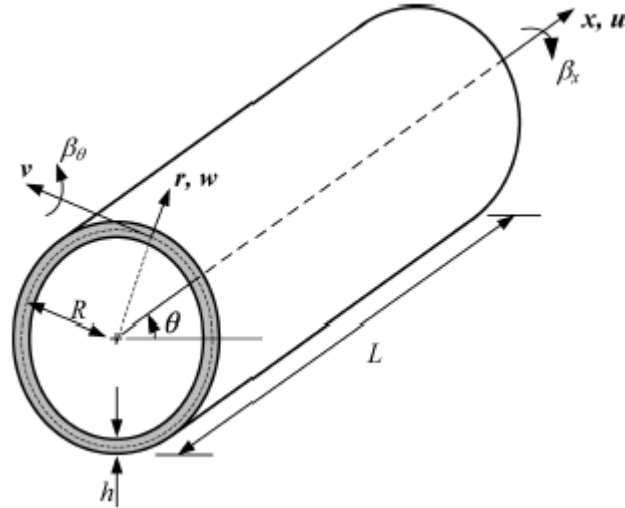


Figure 3.2: Single walled nanotube modeled as a beam or cylindrical shell

Here, $N_{xx}, N_{\theta\theta}, N_{x\theta}$ are in-plane forces: M_{xx} and $M_{x\theta}$ are moments: Q_x and Q_θ are transverse shear forces: w is radial displacement and R is radius of cylindrical shell. And s_1 and s_2 are tracer coefficients which are used for implementing the different shell theories,

- $s_1 = 1$ and $s_2 = 1$ for FSDST

The assumption of shell material is to be isotropic and obeying Hook's law and to the assumptions made the stress-resultants-displacements and strain-displacements relations are:

For FSDST,

$$N_{xx} = C \left[\frac{\partial u}{\partial x} + \frac{\mu}{R} \left(\frac{\partial v}{\partial \theta} + w \right) \right] = 0 \quad (3.43)$$

$$N_{\theta\theta} = C \left[\mu \frac{\partial u}{\partial x} + \frac{1}{R} \left(\frac{\partial v}{\partial \theta} + w \right) \right] = 0 \quad (3.44)$$

$$N_{x\theta} = \frac{C(1-\mu)}{2} + \left(\frac{\partial v}{\partial x} + \frac{1}{R} \frac{\partial u}{\partial \theta} \right) = 0 \quad (3.45)$$

$$M_{xx} = D \left(\frac{\partial \beta_x}{\partial x} + \frac{\mu}{R} \frac{\partial \beta_\theta}{\partial \theta} \right) = 0 \quad (3.46)$$

$$M_{\theta\theta} = D \left(\mu \frac{\partial \beta_x}{\partial x} + \frac{1}{R} \frac{\partial \beta_\theta}{\partial \theta} \right) = 0 \quad (3.47)$$

$$M_{x\theta} = \frac{D(1-\mu)}{2} \left[\frac{\partial \beta_\theta}{\partial x} + \frac{1}{R} \frac{\partial \beta_x}{\partial \theta} + \frac{1}{2R} \left(\frac{\partial v}{\partial x} - \frac{1}{R} \frac{\partial u}{\partial \theta} \right) \right] = 0 \quad (3.48)$$

$$Q_x = k_s Gh \left(\frac{\partial w}{\partial x} + \beta_x \right) \quad (3.49)$$

$$Q_\theta = k_s Gh \left(\frac{1}{R} \frac{\partial w}{\partial \theta} - \frac{\nu}{R} + \beta_\theta \right) \quad (3.50)$$

where K_s is shear correction factor (taken as 5/6): ($C = Eh / (1 - \mu^2)$ and $D = Eh^3 / [12(1 - \mu^2)]$):
 E is young's modulus and G is shear modulus : μ is poisson's ratio : $\{u, v, w\}$ are displacements in (x, θ, r) directions, and $\{\beta_x$ and $\beta_\theta\}$ are rotations about x and θ axes.

In case of donnell thin shell theory (DST) and SST , the constitutive shear forces are zero, because thin shell theories neglect the effect of transverse shear deformation. Therefore, the shear forces in DST and SST are calculated from the equilibrium equations (3.45) and (3.46) . The stress-resultant-displacment are, therefore , only defined for following constitutive stress-resultants:

$$N_{xx} = C \left[\frac{\partial u}{\partial x} + \frac{\mu}{R} \left(\frac{\partial v}{\partial \theta} + w \right) \right] = 0 \quad (3.51)$$

$$N_{\theta\theta} = C \left[\mu \frac{\partial u}{\partial x} + \frac{1}{R} \left(\frac{\partial v}{\partial \theta} + w \right) \right] = 0 \quad (3.52)$$

$$N_{x\theta} = \frac{C(1-\mu)}{2} + \left(\frac{\partial v}{\partial x} + \frac{1}{R} \frac{\partial u}{\partial \theta} \right) = 0 \quad (3.53)$$

$$M_{xx} = -D \left[\frac{\partial^2 w}{\partial x^2} + \frac{\mu}{R^2} \frac{\partial}{\partial \theta} \left(\frac{\partial w}{\partial \theta} - s_2 \nu \right) \right] \quad (3.54)$$

$$M_{\theta\theta} = -D \left[\frac{\partial^2 w}{\partial x^2} + \frac{1}{R^2} \frac{\partial}{\partial \theta} \left(\frac{\partial w}{\partial \theta} - s_2 \nu \right) \right] \quad (3.55)$$

$$M_{x\theta} = -\frac{D(1-\mu)}{2R} \left[\frac{\partial^2 w}{\partial x \partial \theta} + s_2 \left(\frac{\partial^2 w}{\partial x \partial \theta} - \frac{3}{2} \frac{\partial v}{\partial x} + \frac{1}{2R} \frac{\partial u}{\partial \theta} \right) \right] = 0 \quad (3.56)$$

On substitution the stress-resultants relation into equilibrium equation (3.42) and (3.46) the governing equations for buckling of FSDST obtained are :

$$C \frac{\partial}{\partial x} \left[\frac{\partial u}{\partial x} + \frac{\mu}{R} \left(\frac{\partial u}{\partial \theta} + w \right) \right] + \frac{C(1-\mu)}{2R} \frac{\partial}{\partial \theta} \left(\frac{\partial v}{\partial x} + \frac{1}{R} \frac{\partial u}{\partial \theta} \right) - \frac{D(1-\mu)}{4R^2} \frac{\partial}{\partial \theta} \left[\frac{\partial \beta_\theta}{\partial x} + \frac{1}{R} \frac{\partial \beta_x}{\partial \theta} + \frac{1}{2R} \left(\frac{\partial v}{\partial x} - \frac{1}{R} \frac{\partial u}{\partial \theta} \right) \right] = 0 \quad (3.57)$$

$$\begin{aligned} \frac{C(1-\mu)}{2} \frac{\partial}{\partial x} \left(\frac{\partial v}{\partial x} + \frac{1}{R} \frac{\partial u}{\partial \theta} \right) + \frac{D(1-\mu)}{4R} \frac{\partial}{\partial x} \left[\frac{\partial \beta_\theta}{\partial x} + \frac{1}{R} \frac{\partial \beta_x}{\partial \theta} + \frac{1}{2R} \left(\frac{\partial v}{\partial x} - \frac{1}{R} \frac{\partial u}{\partial \theta} \right) \right] \frac{C}{R} \frac{\partial}{\partial \theta} \left[\left(\mu \frac{\partial u}{\partial x} + \frac{1}{R} \left(\frac{\partial v}{\partial \theta} + w \right) \right) \right] \\ + \frac{k_s Gh}{R} \left(\frac{1}{R} \frac{\partial w}{\partial \theta} - \frac{\nu}{R} + \beta_\theta \right) = 0 \end{aligned} \quad (3.59)$$

$$k_s Gh \frac{\partial}{\partial x} \left(\frac{\partial w}{\partial x} + \beta_x \right) + \frac{k_s Gh}{R} \frac{\partial}{\partial \theta} \left(\frac{1}{R} \frac{\partial w}{\partial \theta} - \frac{\nu}{R} + \beta_\theta \right) \frac{C}{R} \left[\left(\mu \frac{\partial u}{\partial x} + \frac{1}{R} \left(\frac{\partial v}{\partial \theta} + w \right) \right) \right] - N \frac{\partial^2 w}{\partial x^2} = 0 \quad (3.60)$$

$$D \frac{\partial}{\partial x} \left(\frac{\partial \beta_x}{\partial x} + \frac{\mu}{R} \frac{\partial \beta_\theta}{\partial \theta} \right) + \frac{D(1-\mu)}{2R} \frac{\partial}{\partial \theta} \left[\frac{\partial \beta_\theta}{\partial x} + \frac{1}{R} \frac{\partial \beta_x}{\partial \theta} + \frac{1}{2R} \left(\frac{\partial v}{\partial x} - \frac{1}{R} \frac{\partial u}{\partial \theta} \right) \right] - k_s Gh \left(\frac{\partial w}{\partial x} + \beta_x \right) = 0 \quad (3.61)$$

$$\frac{D(1-\mu)}{2} \frac{\partial}{\partial x} \left[\frac{\partial \beta_\theta}{\partial x} + \frac{1}{R} \frac{\partial \beta_x}{\partial \theta} + \frac{1}{2R} \left(\frac{\partial v}{\partial x} - \frac{1}{R} \frac{\partial u}{\partial \theta} \right) \right] + \frac{D}{R} \frac{\partial}{\partial \theta} \left(\mu \frac{\partial \beta_x}{\partial x} + \frac{1}{R} \frac{\partial \beta_\theta}{\partial \theta} \right) - \frac{k_s Gh}{R} \left(\frac{1}{R} \frac{\partial w}{\partial \theta} - \frac{\nu}{R} + \beta_\theta \right) = 0 \quad (3.62)$$

The equations mentioned above when solved with appropriate boundary condition give buckling solution (lowest positive eigen value).However , it is very difficult to obtain the exact buckling solution

Chapter 4

Results And Discussion

4.1 Analytical Results

- The continuum model for Carbon nanotube was approximated by considering thickness of 0.066nm [19][19]
- And, for boron nitride nanotube was approximated by considering thickness of 0.065nm [25]
- And, Elastic modulus for BNNT was found to be as 1.24TPa [32],[33]. and for CNT 1TPa. The analytical results were being explained over here for the nanotube under compression and critical compressive force were evaluated from equation as mentioned. The effective length of the nanotube was taken as 4 when ends are clamped.
- The nanotube diameters of zigzag CNT and BNNT configuration were found to be 0.392nm and 0.405nm and for armchair CNT and BNNT were 0.4071nm BNNT 0.4211nm.
- And, from atomistic point of view Bond lengths were reported to be 0.1421nm for CNT and 0.147nm of BNNT.

In present work analytical results for the comparison of armchair and zigzag CNTs with that of armchair and zigzag BNNTs for the different parameter such as aspect ratio , nanotube diameter with critical compressive buckling force has been done for nanotube under axial compression .

4.1.1 Nanotube under compression

Classical Euler formula of cantilever column for critical load :[19]

$$\text{Critical Compressive Buckling Force (nN) } F_{cr} = \frac{\pi^2 EI}{4L^2} \quad (4.1)$$

Moment of inertia :[11]

$$\text{Moment Of inertia} = \frac{\pi(d_o^4 - d_i^4)}{64} \quad (4.2)$$

The calculated critical compressive forces from euler formula as mentioned above from equation 3.64 for increasing aspect ratio and different length are summarised as below in Table 4.1 for armchair (3,3) CNT and in Table4.2 for armchair BNNT

<i>Srno.</i>	<i>A.R</i>	<i>l(nm)</i>	<i>F_{cr}(nN)</i>
1	2	0.8142	3.965778379
2	4	1.6284	0.991444595
3	6	2.4426	0.440642042
4	8	3.2568	0.247861149
5	10	4.071	0.158631135

Table 4.1: Aspect ratios and critical buckling forces for Armchair (3,3) CNT

<i>Srno.</i>	<i>A.R</i>	<i>l(nm)</i>	<i>F_{cr}(nN)</i>
1	2	0.8422	5.129718971
2	4	1.6844	1.282429743
3	6	2.5266	0.569968775
4	8	3.3688	0.320607436
5	10	4.211	0.205188759

Table 4.2: Aspect ratios and critical buckling forces for Armchair(3,3) BNNT

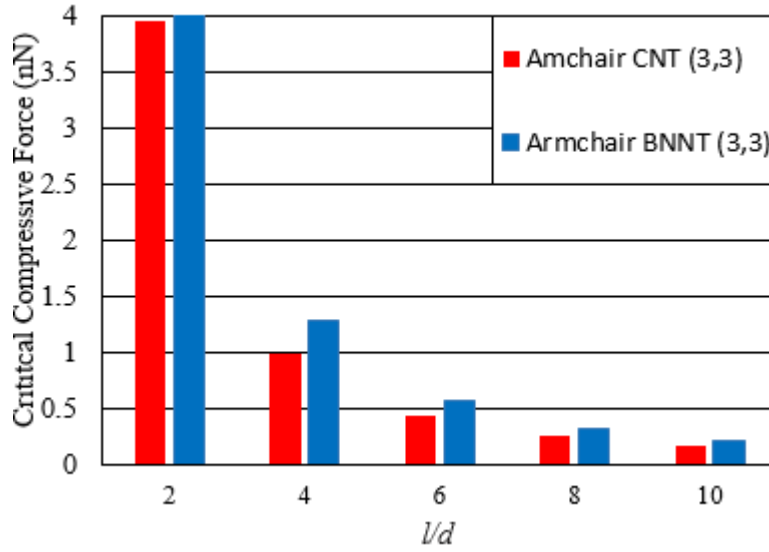


Figure 4.1: Comparison of armchair (3, 3) CNT and BNNT for the effect of nanotube aspect ratio on critical compressive buckling force

It was observed from figure 4.1 that with increase of nanotube aspect ratio buckling force decreases. The buckling force for Armchair CNT decreases more steeply than Armchair of BNNT.

Also for zigzag (5,0) CNT and zigzag(5,0) BNNT calculated critical compressive forces from euler formula as mentioned above from equation 3.64 for increasing aspect ratio and different length are summarised as below in Table 4.3 and for latter in Table 4.4 .

<i>Srno.</i>	<i>A.R</i>	<i>l(nm)</i>	<i>F_{cr}(nN)</i>
1	2	0.7834	3.7423648
2	4	1.5668	0.9355912
3	6	2.3502	0.4158183
4	8	3.1336	0.2338978
5	10	3.917	0.1496946

Table 4.3: Aspect ratios and critical buckling forces for Zigzag(5,0) CNT

<i>Srno.</i>	<i>A.R</i>	<i>l(nm)</i>	<i>F_{cr}(nN)</i>
1	2	0.8104	4.845624
2	4	1.6208	1.211406
3	6	2.4312	0.538403
4	8	3.2416	0.302851
5	10	4.052	0.193825

Table 4.4: Aspect ratios and critical buckling forces for Zigzag(5,0) BNNT

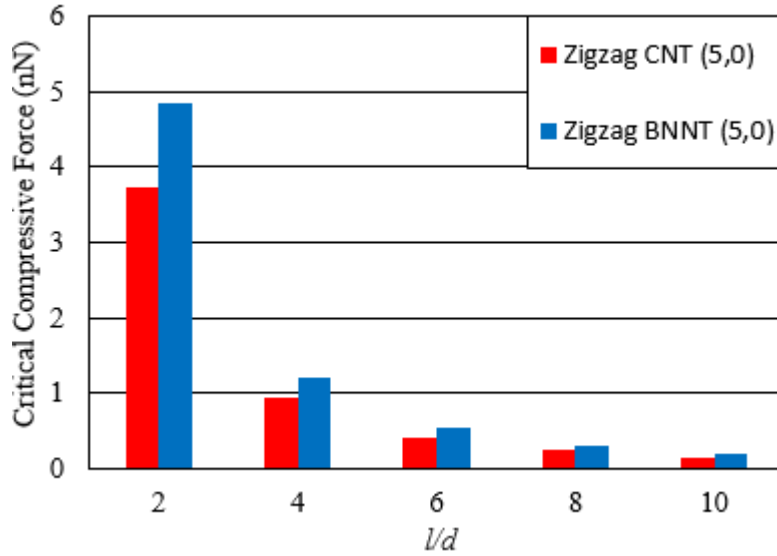


Figure 4.2: Comparison of zigzag (5, 0) CNT and BNNT for the effect of nanotube aspect ratio on critical compressive buckling force

From figure 4.2 the comparison for very small length of aspect ratio 1-2 has been done and it was observed that critical buckling force decreases more steeply for zigzag CNT than BNNT.

$do(nm)$	MOI	$A.R$	$F_{cr}(nN)$
0.268	1.00E-39	4	0.966
0.46	4.00E-39	4	1.714
0.668	1.03E-38	4	2.486
0.868	2.12E-38	4	3.268
0.107	3.79E-38	4	4.055

Table 4.5: Effect of variation in diameter on critical compressive force for armchair CNT

$do(nm)$	MOI	$A.R$	$F_{cr}(nN)$
0.270	9.95E-40	4	1.188279
0.470	3.96E-39	4	2.10366
0.670	1.02E-38	4	3.047329
0.870	2.10E-38	4	4.002973
0.107	3.74E-38	4	4.964793

Table 4.6: Effect of variation in diameter on critical compressive force for armchair BNNT

The nanotube diameters for armchair BNNT and armchair CNT are mentioned above in the table 4.5 and table 4.6 for their increasing effects on nanotubes critical compressive forces.

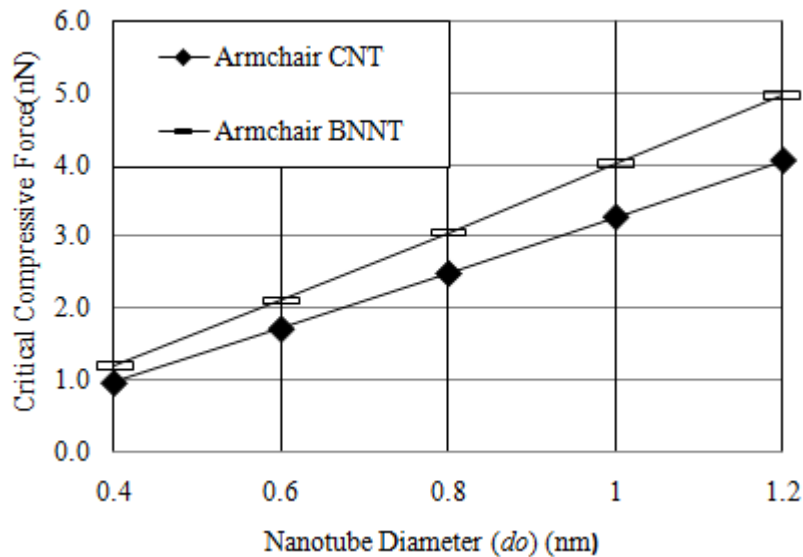


Figure 4.3: Comparison of armchair (3, 3) CNT and BNNT for the effect of nanotube diameter on critical compressive buckling force

Figure 4.3 represents the buckling force results of nanotubes when nanotube diameter is varying. Starting From the small range of 0.4-0.6, the critical buckling force was found to have increasing trend. CNTs were found to have higher values than BNNTs.

As From the above lower critical buckling foces it is infered that nanotubes undergo two buckling modes . The first one is shell buckling mode in which the critical buckling force are found to be higher for smaller length-to-diameter ratio of nanotubes . Further as we go on increasing nanotube aspect ratio the compressive buckling force are found to have lower values and infers that they start exhibiting euler beam buckling mode. And increasing nanotube diameter shows it's linear dependency on critical compressive buckling force.

4.2 Non-local timoshenko beam equations

The small scale effect for the mentioned boundary condition results (analytically) have been computed for the present work . For the effect of small scale

Buckling load relationship between the nonlocal timoshenko tubes and local euler tubes:

$$\frac{P}{EI(1 - \frac{P}{K_sGA}) - (e_0a)^2P} = \frac{P}{EI} \quad (4.3)$$

$$P = \frac{P_E}{1 + \frac{P}{K_sGA} + (e_0a)^2 \frac{P}{EI}} \quad (4.4)$$

Here, P_E is buckling of local euler rod/tube, i.e $P_E = \pi^2 EI/L^2$ for pinned ended rod/tube , $P_E = 4\pi^2 EI/L^2$ for a clamped ended tube and $P_E = 4\pi^2 EI/(4L^2)$ for a clamped-free tube. The buckling load can be determined from solving the equation (76) for lowest positive root The expression (23) for the clamped pinned ended rod may be approximated as:

$$P = \frac{P_E}{1 + 1.1 \frac{P}{K_sGA} + (e_0a)^2 \frac{P}{EI}} \quad (4.5)$$

where ,

$$e_0a = \sqrt{\frac{EI}{K_sGA}} \quad (4.6)$$

From the mentioned parameters results are generated i.e, $E=1\text{TPa}$, $G=E/[2(1+\mu)]$, $\mu=0.19$, rod diameter $d = 1\text{nm}$ and $I = \pi d^4/64$

Local buckling eular load(Pe)	Non-local timoshenko(4.67)	Local timoshenko(4.68)	$(\frac{L}{d})$
0.2411	9.5152	9.5434	10
1.6626	6.7221	6.7543	12
0.1223	4.9621	4.9648	14
0.0936	3.8143	3.8176	16
0.0739	3.0243	3.0267	18
0.0599	2.4221	2.4511	20

Table 4.7: Local buckling eular load(Pe) , Non-local timoshenko and Local timoshenobuckling force P_{cr} (nN) for the clamped-pinned rod for $e_0a = 0$

Local buckling eular load(Pe)	Non-local timoshenko(4.67)	Local timoshenko(4.68)	$(\frac{l}{d})$
0.2411	9.1442	9.1432	10
1.6626	6.4714	6.4933	12
0.1223	4.8416	4.8521	14
0.0936	3.7714	3.7817	16
0.0739	2.9502	2.9415	18
0.0599	2.4752	2.4813	20

Table 4.8: Local buckling eular load(Pe) , Non-local timoshenko and Local timoshenkobuckling forces Pcr(nN) for the clamped-pinned rod for $e_0a = 0.5$

Local buckling eular load(Pe)	Non-local timoshenko(4.67)	Local timoshenko(4.68)	$(\frac{l}{d})$
0.2411	5.2143	5.2332	10
1.6626	4.4201	4.4551	12
0.1223	3.5234	3.5321	14
0.0936	3.2212	3.6721	16
0.0739	2.4201	2.4854	18
0.0599	2.0741	2.0984	20

Table 4.9: Local buckling eular load(Pe) , Non-local timoshenko and Local timoshenko buckling forces Pcr(nN) for the clamped-pinned rod for $e_0a = 2$

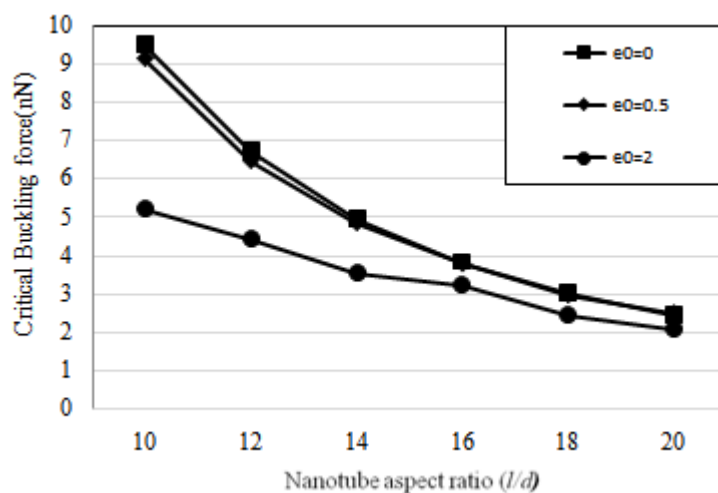


Figure 4.4: Effect of increasing nanotube aspect ratio on critical buckling forces Pcr(nN) for the clamped-pinned rod based on nonlocal Timoshenko beam model

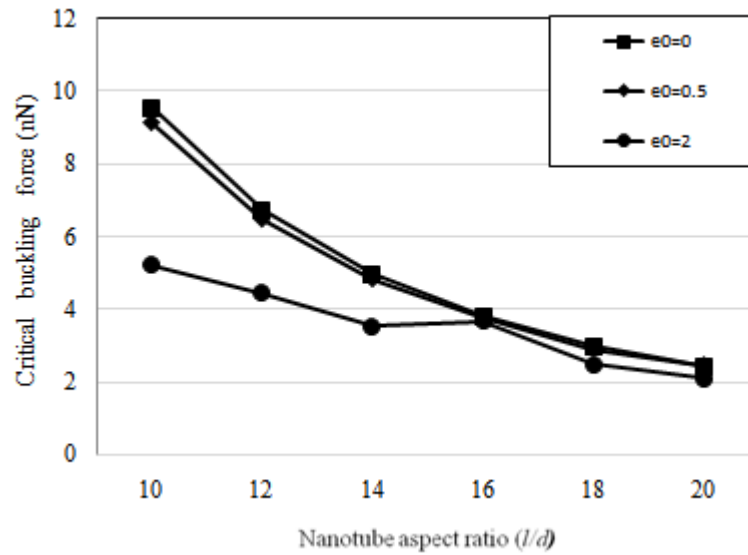


Figure 4.5: Effect of increasing nanotube aspect ratio on critical buckling forces $P_{cr}(nN)$ for the clamped-pinned rod based on on local Timoshenko beam model

It was observed from the figure4.4 and figure4.5, and also by comparing Non-local timoshenko(4.67) and Local timoshenko(4.68) equations that as the scale coefficient increases critical buckling forces were found to be decreasing .

4.3 Nanotubes with different boundary conditions

The effects of nanotube diameter, chirality and boundary condition on buckling force are investigated for nanotubes to study their buckling behaviour in this section. The influence of nanotube aspect ratio and nanotube length are also included to check their dependency on critical buckling strain which are found to be crucial for nanotubes at small or large deformations during compression. However, the continuum model for the simulations were developed in modelling software and eigen buckling analysis was done in ANSYS17.1 for the presented work. The continuum model for the nanotube was developed using effective shell thicknesses, elastic modulus for respective configurations mentioned and poisson's ratio.

Firstly the carbon nanotube has been chosen with effective shell thickness value as, (h) of 0.066nm, young's modulus, (E) taken as 1.06Tpa and poisson's ratio as 0.19.[11][19] And the diameters computed from the equation (1) which accounts for their chirality.

4.3.1 CNT

The critical buckling forces and simulated values of stresses and strains for configurations (8,8),(10,10),(12,12),(15,15) with respective CNT diameters 1.086nm, 1.36nm, 1.63 and 2.04nm for different lengths 15nm, 20nm, 25nm, 30nm of clamped ends are summarised in table 4.10

<i>Chirality</i>	<i>d(nm)</i>	<i>length(l) nm</i>	Critical force(nN)	Stress (σ)	Strain (ϵ)
(8,8)	1.086	15	0.321	57.141	0.054
		20	0.115	28.485	0.026
		25	0.180	179.593	0.017
		30	0.080	12.953	0.012
(10,10)	1.36	15	0.649	403.184	0.381
		20	0.365	377.345	0.002
		25	0.234	23.535	0.023
		30	0.162	20.394	0.019
(12,12)	1.63	15	1.150	404.523	0.382
		20	0.646	278.541	0.263
		25	0.413	265.05	0.251
		30	0.287	18.875	0.017
(15,15)	2.04	15	2.300	264.66	0.250
		20	1.291	190.423	0.180
		25	0.828	179.15	0.169
		30	0.575	164.85	0.156

Table 4.10: Geometrical parameters and buckling forces for clamped CNTs

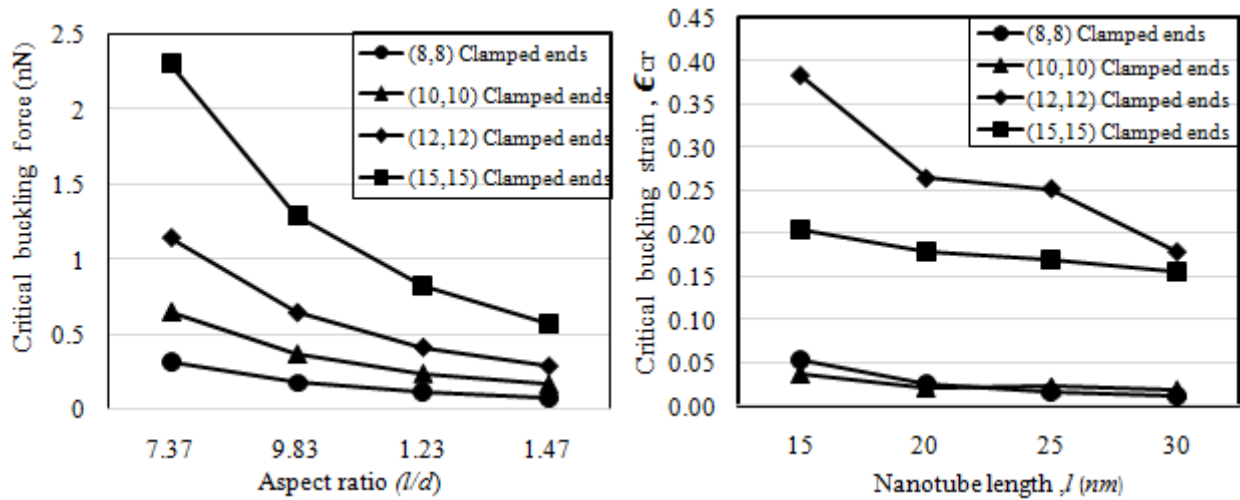


Figure 4.6: Effect of nanotube aspect ratio on critical compressive buckling force and critical buckling strain for clamped ends (armchair CNTs)

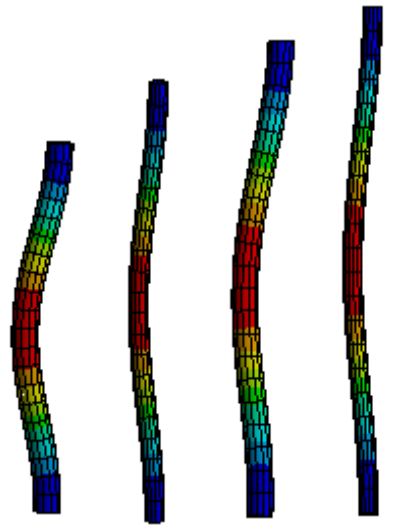


Figure 4.7: Deformed configurations of (8,8) CNT with deformations 1.23nm, 1.06nm , 1.02nm , 1.0nm after eigen buckling of lengths $l = 15, 20, 25, 30nm$ of clamped-ends

Here, critical buckling forces and simulated values of stresses and strains for configurations (8,8),(10,10),(12,12),(15,15) with respective CNT diameters 1.086nm , 1.36nm 1.63 and 2.04nm for different lengths 15nm,20nm ,25nm, 30nm of pinned ends are summarised in table 4.11

Chirality	d (nm)	length(l) nm	Critical force(nN)	Stress (σ)	Strain (ε)
(8,8)	1.086	15	1.28	150.00	0.164
		20	0.0721	981.04	0.103
		25	0.462	841.04	0.926
		30	0.321	371.01	0.406
(10,10)	1.36	15	2.60	329.58	0.343
		20	1.16	174.96	0.187
		25	0.935	115.22	0.123
		30	0.649	71.065	0.078
(12,12)	1.63	15	4.59	845.00	0.815
		20	2.58	229.00	0.242
		25	1.65	135.00	0.143
		30	1.15	94.181	0.100
(15,15)	2.04	15	9.20	686.00	0.678
		20	5.17	592.00	0.567
		25	3.31	501.00	0.481
		30	2.30	113.00	0.121

Table 4.11: Geometrical parameters and buckling forces for Pinned CNTs

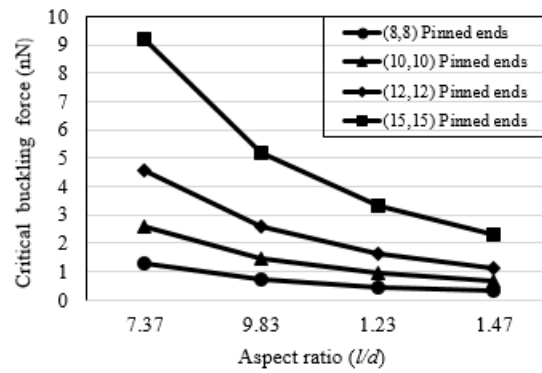


Figure 4.8: Effect of nanotube aspect ratio on critical compressive buckling force and critical buckling strain for pinned ends (armchair CNTs)

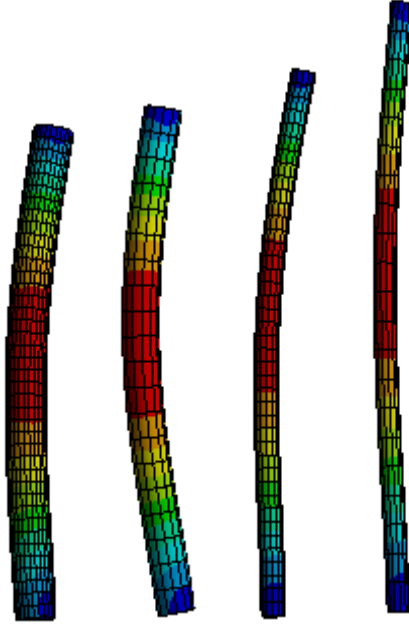


Figure 4.9: Deformed configurations of (8,8) CNT with deformations 1.00nm, 1.01nm , 1.00nm , 1.00nm after eigen buckling of lengths $l = 15, 20, 25, 30nm$ of pinned-ends

Critical buckling forces and simulated values of stresses and strains for configurations (8,8),(10,10),(12,12),(15,15) with respective CNT diameters 1.086nm , 1.36nm 1.63 and 2.04nm for different lengths 15nm,20nm ,25nm, 30nm of clamped-free ends are summarised in table 4.12

<i>Chirality</i>	<i>d(nm)</i>	<i>length(l) nm</i>	Critical buckling force(nN)	Stress (σ)	Strain (ϵ)
(8,8)	1.086	15	5.13	6.410	0.006
		20	2.89	3.570	0.003
		25	1.85	2.310	0.002
		30	1.28	1.830	0.001
(10,10)	1.36	15	1.04	108.7	0.010
		20	5.84	4.433	0.004
		25	3.74	2.848	0.002
		30	2.60	2.006	0.001
(12,12)	1.63	15	1.84	56.990	0.010
		20	1.03	32.149	0.005
		25	6.62	3.574	0.003
		30	4.59	3.480	0.003
(15,15)	2.04	15	3.68	12.363	0.011
		20	2.07	730.6	0.006
		25	1.32	5.400	0.005
		30	9.20	2.9654	0.00280

Table 4.12: Geometrical parameters and buckling forces for clamped-free CNTs

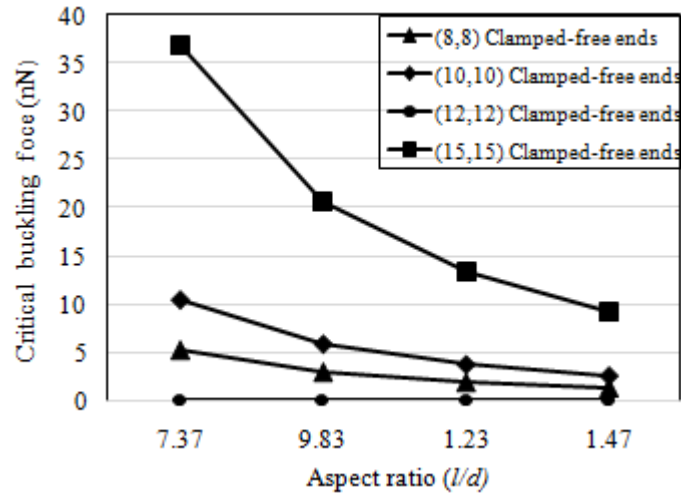


Figure 4.10: Effect of nanotube aspect ratio on critical compressive buckling force and critical buckling strain for clamped-free ends (armchair CNTs)

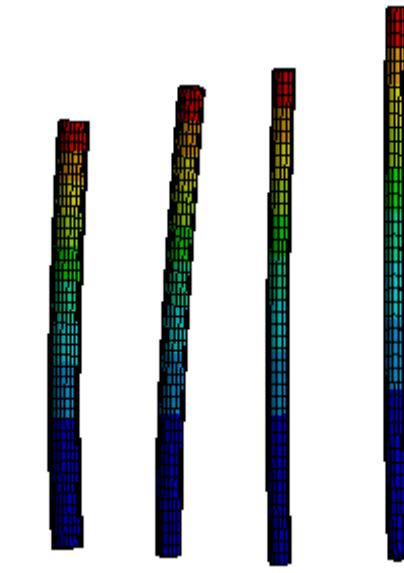


Figure 4.11: Deformed configurations of (8,8) CNT with deformations 1.00nm, 1.01nm , 1.00nm , 1.13nm after eigen buckling of lengths $l = 15, 20, 25, 30nm$ of clamped-free ends

- From the tables and figures above it was observed that the critical buckling forces decreases with the mentioned boundary conditions for the same aspect ratios but for clamped ends compressive buckling forces decreases more rapidly .
- And critical buckling strains were found to be decreasing for clamped ends , whereas for pinned ends and some configurations of clamped-free were having different trend of strains. Therefore, the parameter nanotube length is found to be sensitive to tube chirality's and chosen different boundary conditions for CNTs.

4.3.2 BNNT

Secondly, the boron nitride nanotube has been chosen with effective shell thickness value as, (h) of 0.065nm , young's modulus, (E) taken as 1.24Tpa and poisson's ratio as 0.35.

The Critical buckling forces and simulated values of stresses and strains for configurations (8,8),(10,10),(12,12),(15,15) with respective BNNT diameters 1.1236nm , 1.40nm 1.68 and 2.11nm for different lengths 15nm,20nm ,25nm, 30nm of clamped ends are summarised in table 4.13

Chirality	$d(nm)$	length(l) nm	Critical force(nN)	Stress (σ)	Strain (ϵ)
(8,8)	1.123	15	4.12	707.15	0.571
		20	2.32	4.7758	0.003
		25	1.48	2.8070	0.002
		30	1.03	3.7374	0.003
(10,10)	1.40	15	8.33	470.65	0.380
		20	4.69	2526.7	0.002
		25	3.00	2309.3	0.001
		30	2.08	2017.6	0.001
(12,12)	1.68	15	1.47	343.19	0.277
		20	8.29	449.42	0.363
		25	5.31	371.96	0.300
		30	3.69	303.66	0.330
(15,15)	2.11	15	2.95	219.49	0.177
		20	1.66	286.28	0.231
		25	1.06	198.35	0.160
		30	7.37	182.05	0.148

Table 4.13: Geometrical parameters and buckling forces for clamped end BNNTs

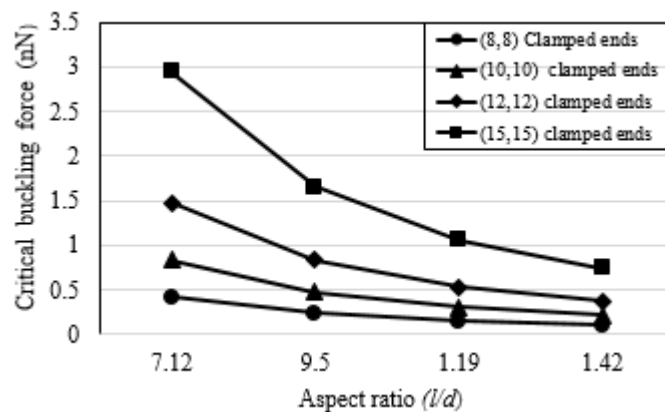


Figure 4.12: Effect of nanotube aspect ratio on critical compressive buckling force and critical buckling strain for clamped ends (armchair BNNTs)

Critical buckling forces and simulated values of stresses and strains for configurations (8,8),(10,10),(12,12),(15,15) with respective BNNT diameters 1.1236nm , 1.40nm 1.68

and 2.11nm for different lengths 15nm,20nm ,25nm, 30nm of pinned ends are summarised in table 4.14

Chirality	$d(nm)$	length(l) nm	Critical force(nN)	Stress (σ)	Strain (ϵ)
(8,8)	1.123	15	1.65	48.139	0.0388
		20	9.27	27.006	0.021
		25	5.93	16.459	0.013
		30	4.12	12.523	0.010
(10,10)	1.40	15	3.33	75.827	0.051
		20	1.88	32.995	0.026
		25	1.20	20.924	0.016
		30	8.33	15.137	0.012
(12,12)	1.68	15	5.90	83.552	0.067
		20	3.32	39.787	0.032
		25	2.12	17.222	0.024
		30	1.47	17.221	0.013
(15,15)	2.11	15	1.18	166.56	0.114
		20	6.63	49823	0.040
		25	4.24	29.334	0.023
		30	2.95	20.759	0.016

Table 4.14: Geometrical parameters and buckling forces for pinned end BNNTs

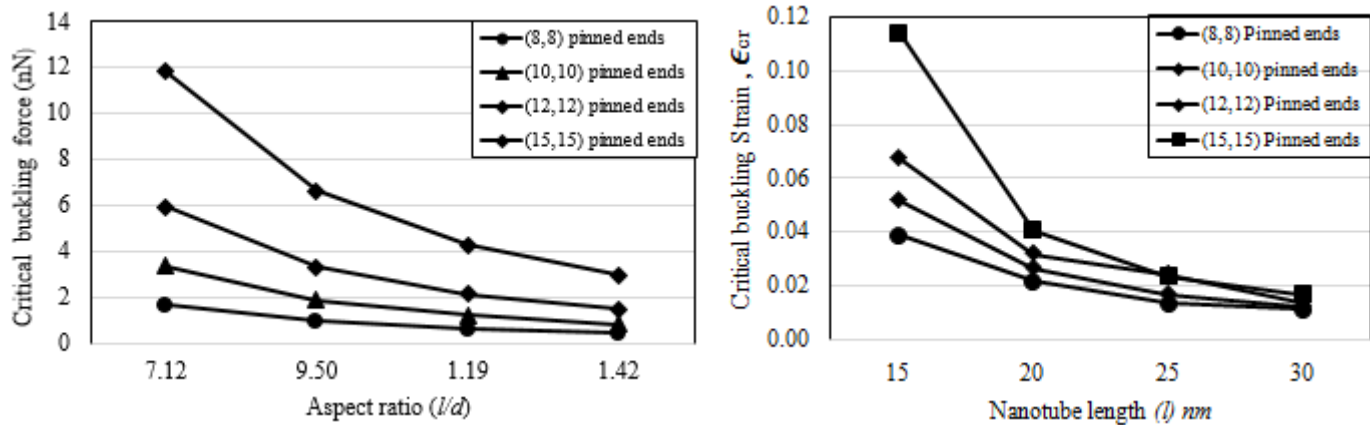


Figure 4.13: Effect of nanotube aspect ratio on critical compressive buckling force and critical buckling strain for pinned ends (armchair BNNTs)

Critical buckling forces and simulated values of stresses and strains for configurations (8,8),(10,10),(12,12),(15,15) with respective BNNT diameters 1.1236nm , 1.40nm 1.68 and 2.11nm for different lengths 15nm,20nm ,25nm, 30nm of clamped-free ends are summarised in table 4.15

Chirality	d (nm)	length(l) nm	Critical force(nN)	Stress (σ)	Strain (ϵ)
(8,8)	1.123	15	6.59	7.860	0.063
		20	3.71	4.808	0.003
		25	2.37	2.807	0.002
		30	1.65	2.968	0.002
(10,10)	1.40	15	1.33	9.884	0.007
		20	7.50	5.852	0.004
		25	4.80	4.003	0.003
		30	3.33	4.135	0.002
(12,12)	1.68	15	2.36	12.858	0.001
		20	1.33	6.151	0.004
		25	8.49	4.204	0.003
		30	5.90	3.075	0.002
(15,15)	2.11	15	4.72	15.231	0.012
		20	2.65	8.686	0.007
		25	1.70	7.197	0.005
		30	1.18	4.445	0.003

Table 4.15: Geometrical parameters and buckling forces for clamped-free BNNTs

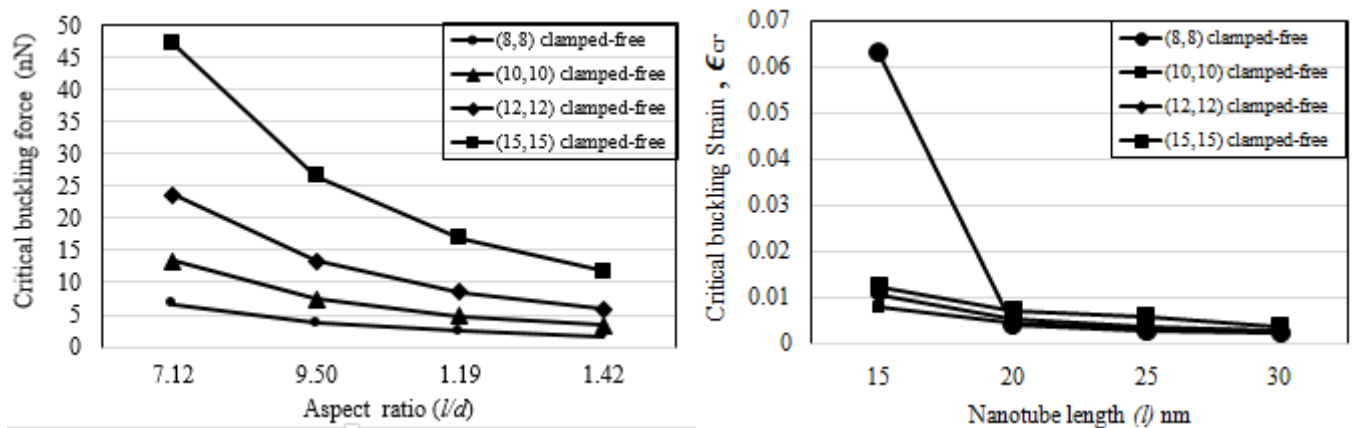


Figure 4.14: Effect of nanotube aspect ratio on critical compressive buckling force and critical buckling strain for clamped-free ends (armchair BNNTs)

- From figures 4.12, 4.13 and 4.14 above it was observed that the critical buckling forces decreases rapidly with the mentioned boundary conditions for the same aspect ratios but for clamped ends compressive buckling forces decreases more rapidly.
- And critical buckling strains were found to be consistently decreasing for pinned ends and clamped-free ends. Therefore, the parameter nanotube length is found to be sensitive to tube chirality's and chosen different boundary conditions for BNNTs also.

4.4 critical bending buckling strain

In order to further explore the diameter-dependence for the constrained boundary effect critical bending buckling strain are investigated for varied armchair and zigzag configurations. Here, the length for the said configuration of nanotubes was chosen to be 8nm. And The critical compressive buckling strain of axially compressed shell is given by: [15],[17][34]

The critical bending buckling strain was computed analytically by given formula and simulated by eigen value buckling analysis .

$$\varepsilon_{cr-comp}^{shell} = \frac{2}{\sqrt{3(1-\nu^2)}} \frac{t}{d} \quad (4.7)$$

Simulated critical strain values and calculated critical strain values for configurations (8,8) , (10,10) , (12,12) and (15,15) of CNTs and BNNTs are mentioned in table 4.16 and table 4.17

Chirality	$d(nm)$	$\varepsilon_{cr}(Analytical)$	$\varepsilon_{cr}(Simulated)$
(8,8)	1.09	0.0714	0.0718
(10,10)	1.36	0.0572	0.0605
(12,12)	1.63	0.0477	0.0480
(15,15)	2.04	0.0381	0.0395
(17,17)	2.31	0.0336	0.0360
(20,20)	2.71	0.0286	0.0305
(23,23)	3.12	0.0249	0.0260

Table 4.16: Geometrical parameters and critical strain value for armchair CNT

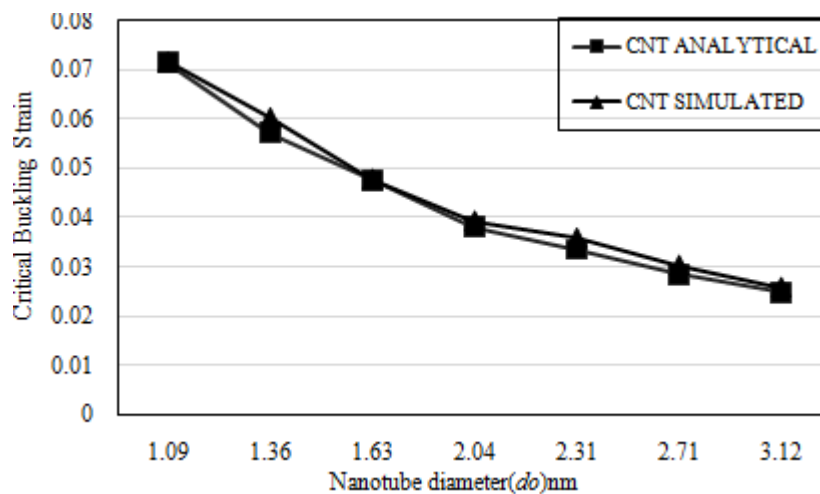


Figure 4.15: Comparison of simulated and analytical buckling strains of armchair configurations CNT for the effect of nanotube diameter

<i>Chirality</i>	<i>d(nm)</i>	$\varepsilon_{cr}(Analytical)$	$\varepsilon_{cr}(Simulated)$
(8,8)	1.12	0.0713	0.0713
(10,10)	1.40	0.0571	0.0601
(12,12)	1.68	0.0476	0.0476
(15,15)	2.11	0.0381	0.0391
(17,17)	2.39	0.0336	0.0356
(20,20)	2.81	0.0285	0.0301
(23,23)	3.23	0.0248	0.0256

Table 4.17: Geometrical parameters and critical strain value for armchair BNNT

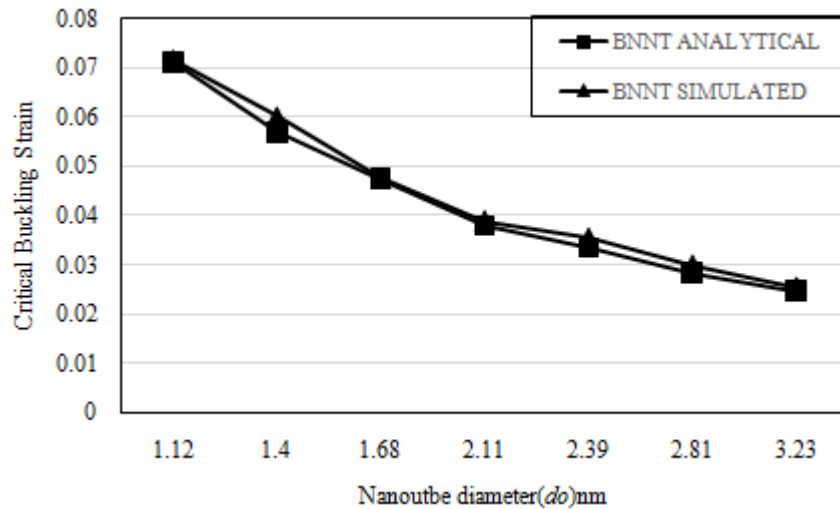


Figure 4.16: Comparison of simulated and analytical buckling strains of armchair configurations BNNT for the effect of nanotube diameter

From the figure 4.15 and 4.16 it was observed that the simulations were found to be consistent with calculated strains and increasing nanotube diameter results in decrease of bending buckling strain for carbon and boron nitride nanotubes . But on comparison part for both nanotubes BNNT decreases more rapidly than CNT.

4.5 Examination of shell theory

- The first shear deformation shell theory has been examined over here on the basis of critical buckling strains and buckling modes of carbon nanotubes from small-to-intermediate to large aspect ratio for various armchair and zigzag configurations used for Clamped ends conditions for capturing the length dependence for varied aspect ratios .
- The foregoing equations mentioned for FSDST are to be solved together for the buckling load (i.e the lowest positive eigen value).

- Generally, it is difficult to obtain the exact buckling solution for cylindrical shells and hence the numerical finite element method is for the solutions .
- Therefore, for the FSDST , the eight node quadrilateral thick shell element with reduced integration S8R , in software ABAQUS, has been used for the present work for the prediction of critical buckling strains.
- For the clamped boundary condition used , the displacements and end rotations are constrained from moving of the cylindrical shell model used .
- The elastic properties such as elastic modulus , poisson's ratio and shell thickness for FSDST model for the computation were 5.5Tpa , 0.19 and 0.066nm.

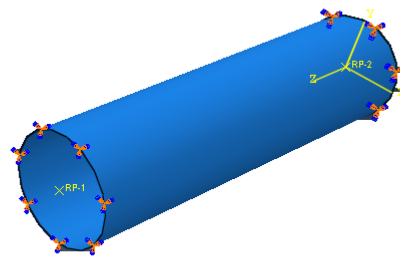


Figure 4.17: Clamped-ends boundary condition for (12,0)

- The mesh of the cylindrical shell comprises of 30 elements along the circumferential length.

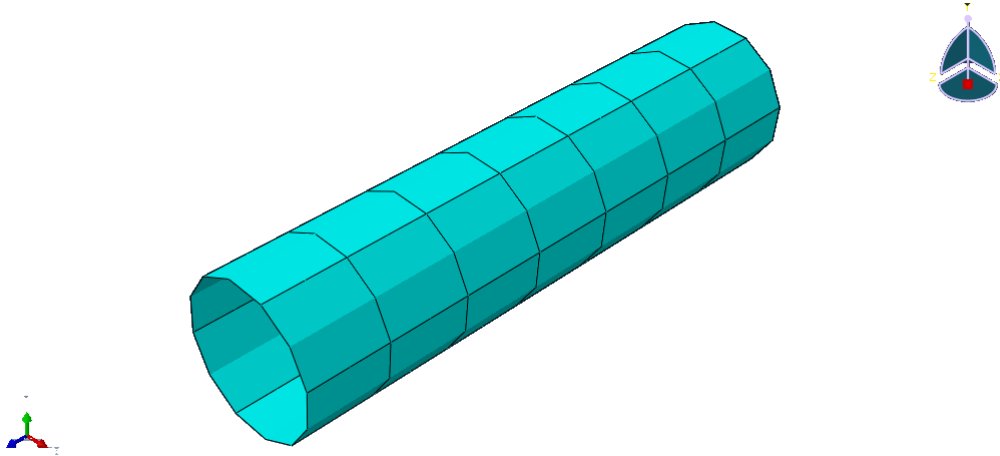


Figure 4.18: mesh design for cylindrical shell (at least 30 elements along circumferential length)

Chirality	$l(nm)$	$d(nm)$	$\frac{l}{d}$	FSDST	Published data
(8,8)	3.3	1.08	3.06	0.925	0.0639
(10,10)	4.1	1.35	3.04	0.740	0.0429
(12,12)	4.8	1.62	2.96	0.617	0.0373
(14,14)	5.7	1.89	3.02	0.529	0.0321
(16,16)	6.4	2.17	2.95	0.460	0.0285
(17,17)	17.8	2.31	7.7	0.409	0.006
(18,18)	7.3	2.44	2.99	0.369	0.025
(20,20)	8.0	2.71	2.95	0.432	0.022
(12,12)	11.2	1.62	6.91	0.617	0.041
(21,0)	11.2	1.65	6.79	0.606	0.047
(8,8)	6.3	1.09	5.78	0.173	0.056
(7,7)	6.0	0.95	6.32	0.158	0.049
(8,0)	4.3	0.63	6.83	1.587	0.120
(20,20)	13.6	2.71	5.02	0.369	0.020
(20,20)	135.7	2.71	50.07	0.369	0.003
(12,0)	2.63	0.94	2.80	1.063	0.064
	2.48		3.70	1.063	0.059
	7.75		8.24	1.063	0.047
	16.27		17.31	1.063	0.016
	31.20		33.19	1.063	0.005

Table 4.18: Critical buckling strains for armchair and zigzag configurations

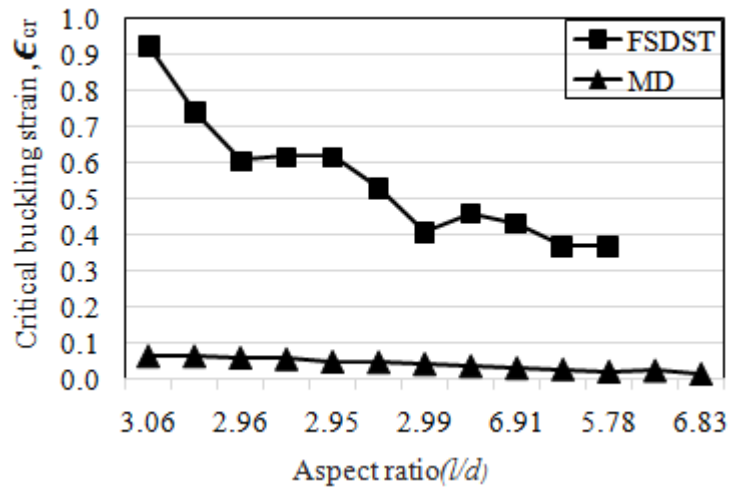


Figure 4.19: Comparison of critical buckling strains for various aspect ratios

- For a better visualisations of the variations of critical buckling strains with respect to aspect ratios l/d , the results are plotted in fig.4.19 and fig 4.20 .
- From figure 4.19 it is inferred that critical buckling strain decreases as the aspect ratios of carbon nanotube get larger .
- For CNTs with lower aspect ratios , the critical buckling strains given by MD results are lower than FSDST model .

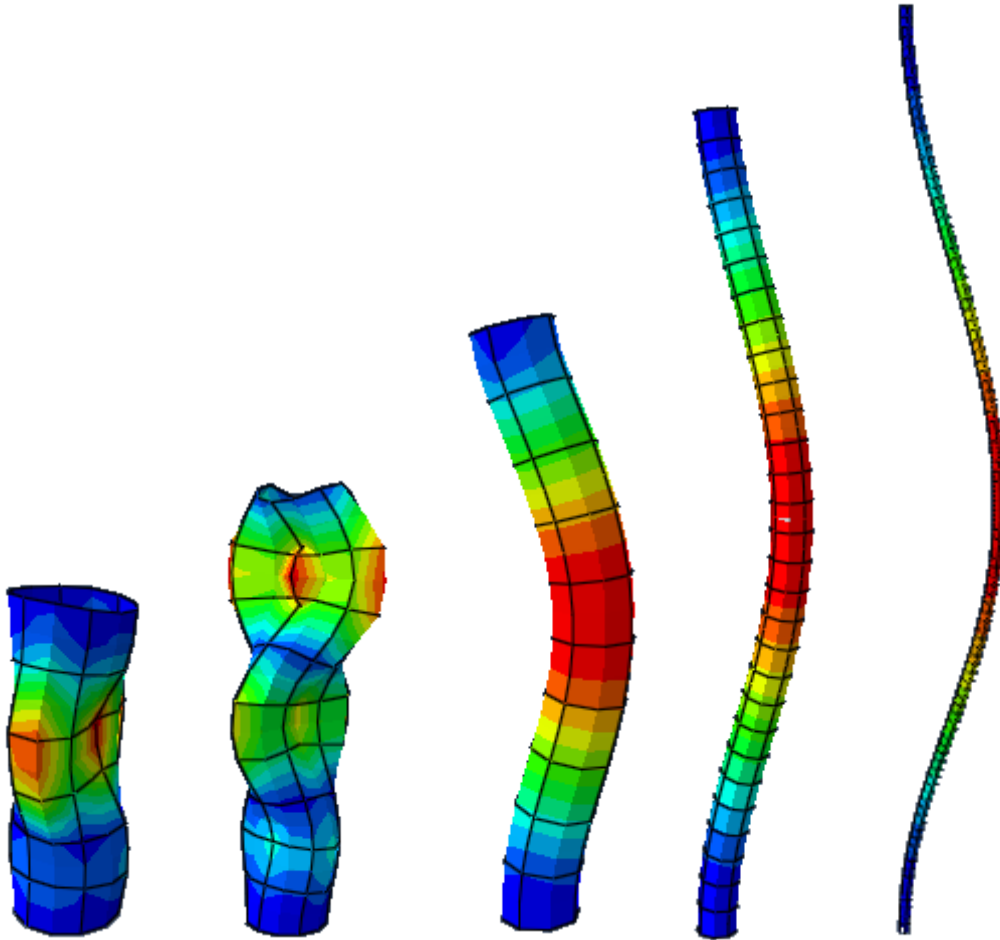


Figure 4.20: Buckling modes of zigzag CNT (12,0) with different aspect ratios $l/d = 2.63, 3.48, 7.75, 16.27, 31.20$ using FSDST

4.6 Nanotubes with different boundary conditions using FSDST

Clamped-clamped	Simply supported	Clamped-free	$\frac{l}{d}$
0.08405	0.0726	0.03472	2.4
0.07956	0.06915	0.02621	3.14
0.07637	0.05108	0.01567	4.24
0.073	0.02862	0.00804	6.08
0.05641	0.01797	0.00481	7.93
0.031	0.00899	0.00229	11.62
0.1915	0.00518	0.00131	15.31
0.01577	0.00416	0.00108	17.15
0.00691	0.00178	0.00175	26.37
0.00386	0.000981	0.00091	35.59
0.00169	0.000434	0.00044	54.03

Table 4.19: Crititcal buckling strains for different boundary condition for armchair (5,5) configuration

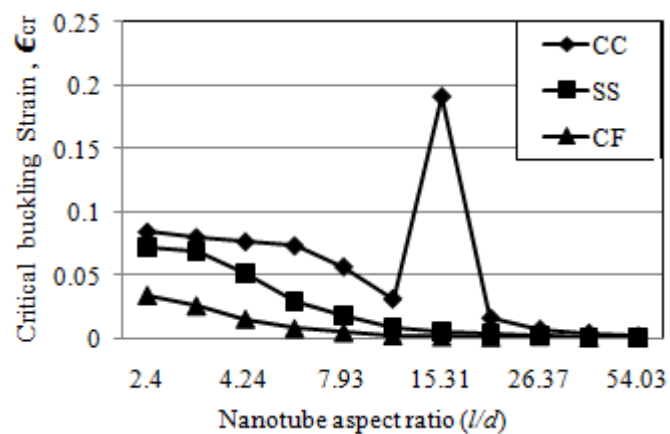


Figure 4.21: Effect of nanotube aspect ratio on critical buckling strain of (5,5) for different boundary conditions

Clamped-clamped	Simply supported	clamped-free	$\frac{l}{d}$
0.06373	0.05202	0.02387	3.01
0.05716	0.04977	0.01506	4.32
0.05456	0.02353	0.00927	5.63
0.0529	0.02272	0.06623	6.93
0.05183	0.01646	0.00449	8.24
0.04242	0.01269	0.00337	9.55
0.02852	0.00807	0.00208	12.17
0.01319	0.00346	0.00089	18.71
0.00748	0.00194	0.00045	25.25
0.00479	0.00121	0.00032	31.79
0.00186	0.00047	0.00011	51.41

Table 4.20: Critical buckling strains for different boundary condition for armchair (7,7) configuration

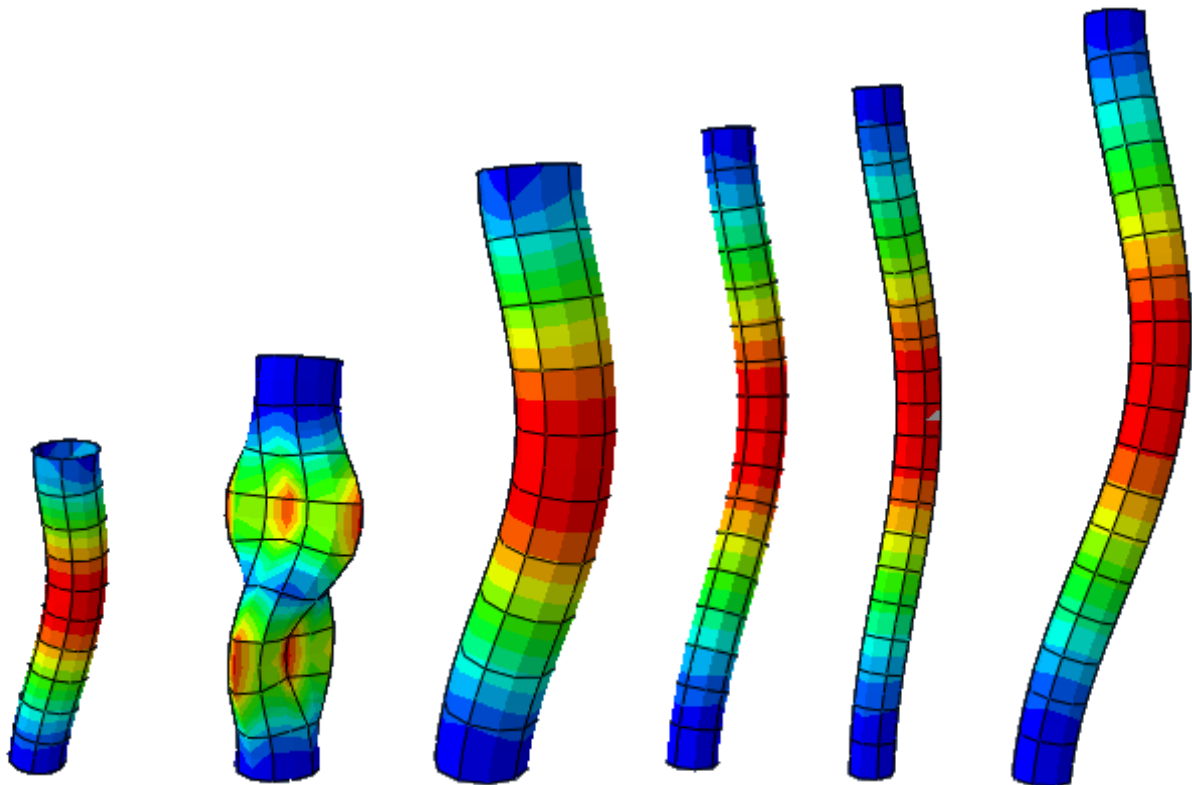


Figure 4.22: Buckling modes of (7,7) CNT for aspect ratios 3.01, 4.32 , 5.63 , 6.93 , 8.24 , 9.55 of clamped boundary condition

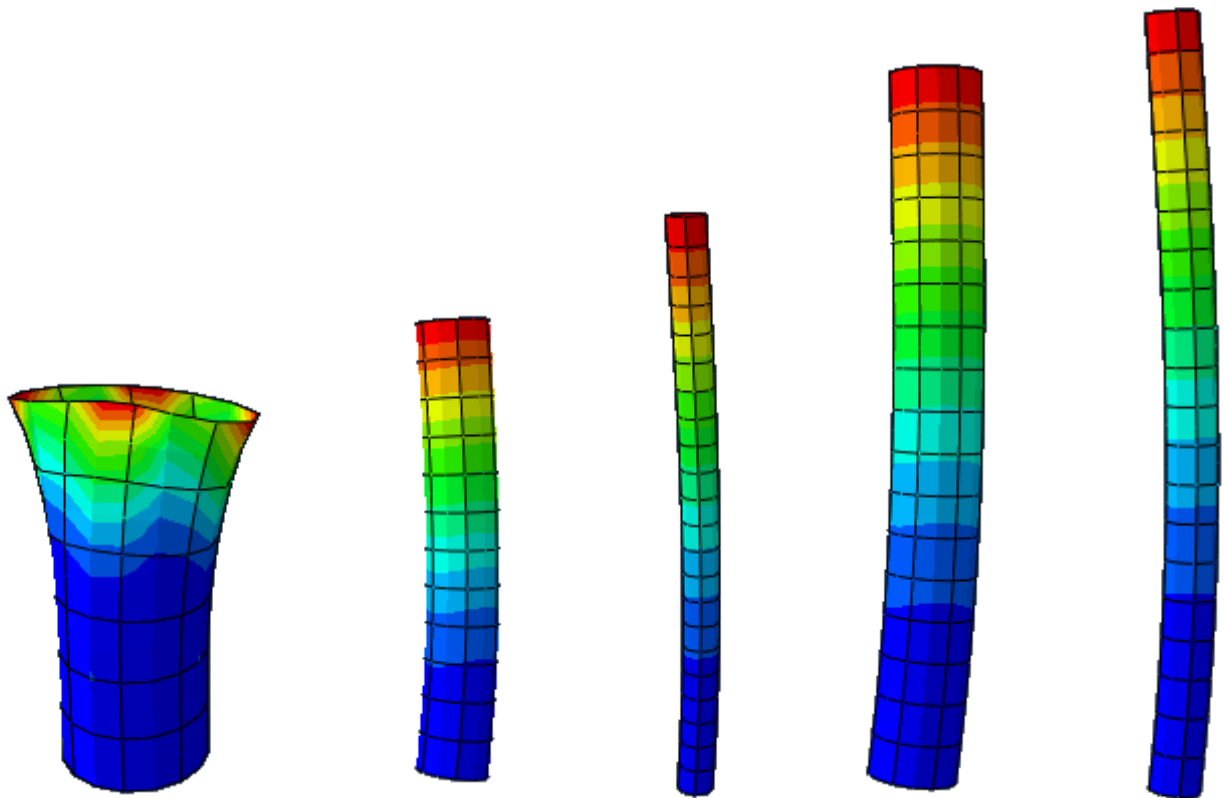


Figure 4.23: Buckling modes of (7,7) CNT for aspect ratios 3.01, 4.32 , 5.63 , 6.93 , 8.24 of clamped-free boundary condition

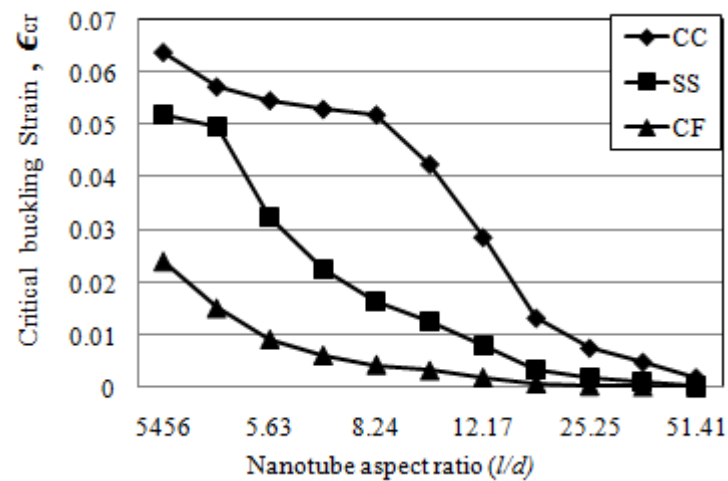


Figure 4.24: Effect of nanotube aspect ratio on critical buckling strain of (7,7) for different boundary conditions

Clamped-clamped	Simply supported	Clamped-free	$\frac{l}{d}$
0.04812	0.03665	0.01684	3.04
0.04410	0.03747	0.01622	4.44
0.04019	0.02973	0.00838	5.93
0.03723	0.01446	0.00381	8.89
0.02425	0.00672	0.00171	13.33
0.01247	0.00329	0.00082	19.26
0.00701	0.00182	0.00044	25.93
0.0042	0.00102	0.00026	34.81
0.00295	0.00075	0.00020	40.74
0.00236	0.0007	0.00014	45.19
0.00278	0.00047	0.00012	50.37

Table 4.21: Critical buckling strains for different boundary condition for armchair (10,10) configuration

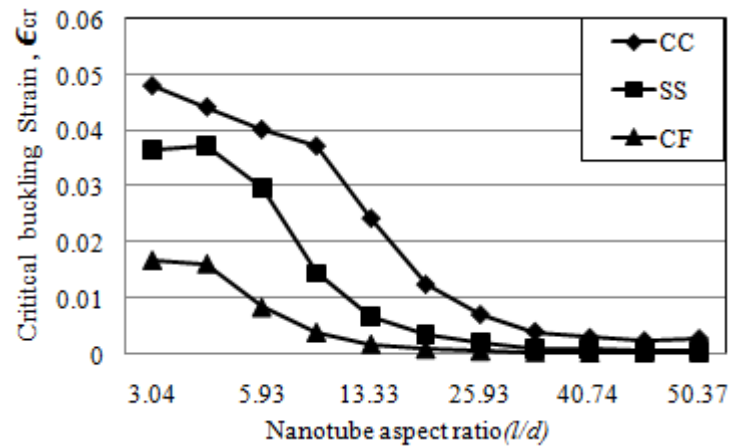


Figure 4.25: Effect of nanotube aspect ratio on critical buckling strain of (10,10) for different boundary conditions

Clamped-clamped	Simply supported	Clamped-free	$\frac{l}{d}$
0.04026	0.02932	0.01420	3.03
0.03784	0.02982	0.01361	4.85
0.03237	0.02013	0.00525	7.27
0.02328	0.00981	0.00237	10.91
0.01722	0.00467	0.00149	15.76
0.00952	0.00245	0.00068	21.82
0.00547	0.00151	0.00037	29.09
0.00343	0.0001	0.00032	36.36
0.00278	0.0006	0.00019	41.21
0.00210	0.00055	0.00015	46.06
0.00184	0.00047	0.00018	50.91

Table 4.22: Critical buckling strains for different boundary condition for armchair (12,12) configuration

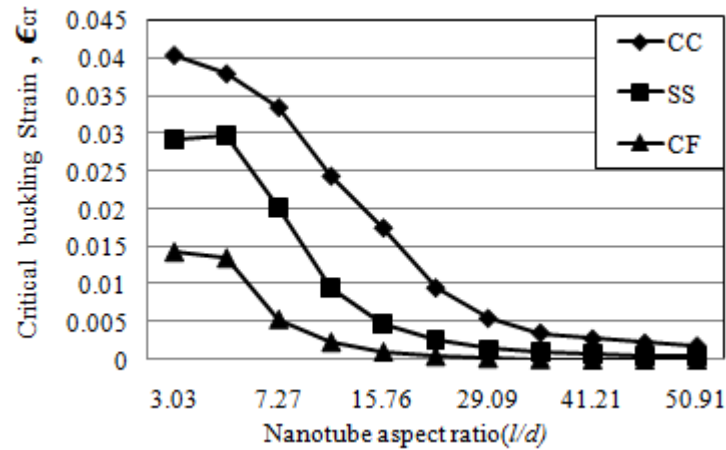


Figure 4.26: Effect of nanotube aspect ratio on critical buckling strain of (12,12) for different boundary conditions

4.7 CNT and BNNT Non-linear response

- The non-linear mechanical response of the nanotube, is said to be as their “buckling” behavior, And, Buckling is a deformation process in which a large strain energy causes an abrupt change in the deformation profile.
- For the non-linear response of SWCNT and SWBNNT the armchair (8,8) chirality was chosen with appropriate parameters such as young’s modulus $E=1.06\text{Tpa}$, [17] and for the latter $E=1.24\text{Tpa}$ [34] in consideration with effective thickness as 0.066nm and 0.065nm with the poisson’s ratio as $\mu=0.19$ for CNT and $\mu=0.35$ for BNNT.
- Also, the zigzag (13,0) SWCNT was chosen for the non-linear response.
- For the computation of stresses, strain, strain energy and deformations of nanotubes the FEM analysis of the model developed was carried out under axial compression. The end rotations and displacements were constrained. The deformations of CNT and BNNT are shown below in Fig4.28 and Fig4.29
- Tables 4.23 and table 4.24 summarizes the values of stresses, strains, deformations and length for (8,8) CNT and (8,8) BNNT.

Chirality	$d(\text{nm})$	length(l) nm	Deformations(nm)	Stress (σ)	Strain (ϵ)
(8,8)	1.086	15	1.23	57.14	0.0543
		20	1.06	28.485	0.0269
		25	1.02	179..59	0.0170
		30	1.01	12.953	0.0122

Table 4.23: Stresses and strains for different lengths of (8,8) for clamped CNT

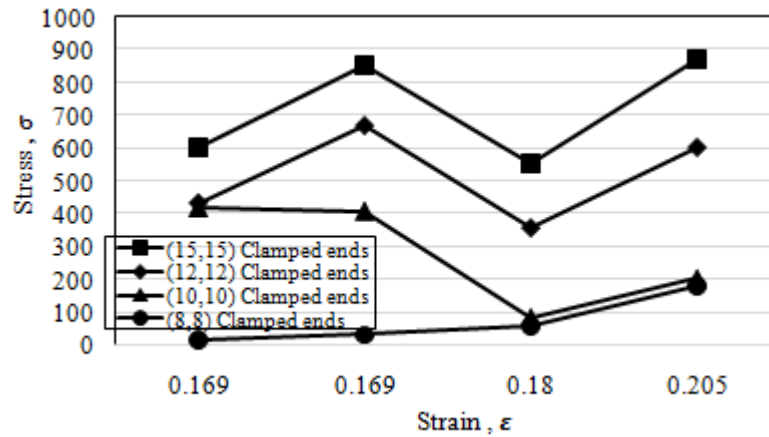


Figure 4.27: Stresses and strains for (8,8) CNT for clamped-ends

When the simulated stresses and strain for configurations (8,8) , (10,10) , (12,12) and (15,15) CNT for the constrained boundary condition were plotted , they were found to have follow non-linear effect. Therefore, the work was done on the non-linear response of CNT and BNNT.

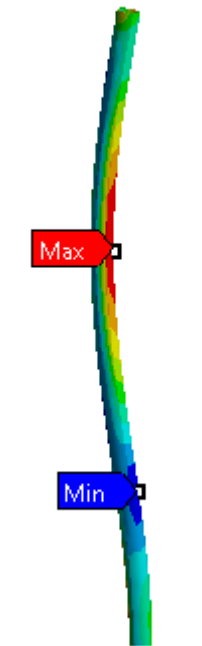


Figure 4.28: Buckled geometrical configuration of (8,8) CNT

The maximum deformation for (8,8) CNT computed by simulations was found to be 1.0024nm approaching the beam buckling behavior .

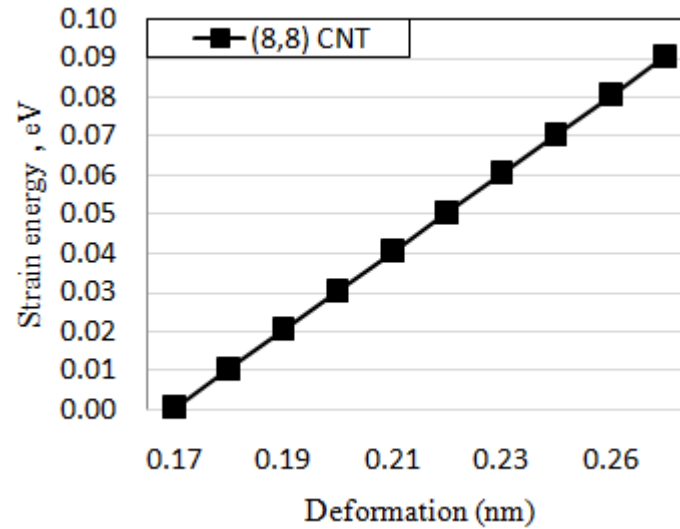


Figure 4.29: Strain energy v/s deformation profile for (8,8) CNT

linearity was found when strain energy and deformations were plotted against each other and it resulted that buckling has said to have occurred for (8,8) CNT.

Chirality	$d(nm)$	length(l) nm	Deformations(nm)	Stress (σ)	Strain (ϵ)
(8,8)	1.123	15	1.06	707.15	0.57
		20	1.10	4.7758	0.00386
		25	1.01	2.807	0.00227
		30	1.00	3.7374	0.00302

Table 4.24: Stresses and strains for different lengths of (8,8) for clamped BNNT

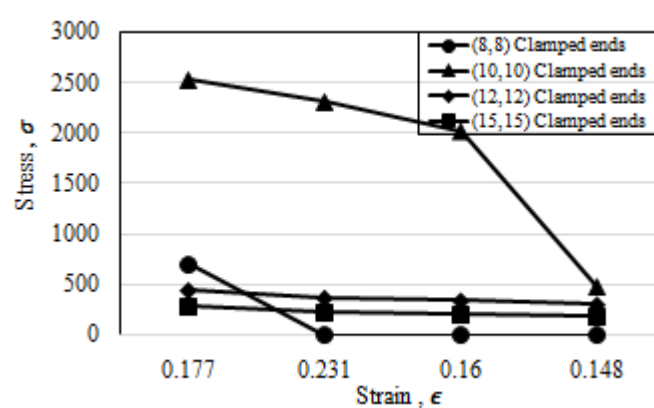


Figure 4.30: Stresses and strains for (8,8) CNT for clamped-ends

Even when the simulated stresses and strain for configurations (8,8) , (10,10) , (12,12) and (15,15) BNNT for the constrained boundary condition were plotted , they were also found to have follow non-linear effect.



Figure 4.31: Buckled geometrical configuration of (8,8) BNNT

The maximum deformation for (8,8) BNNT computed by simulations was found to be 3.7016 nm approaching the beam buckling behavior as like it is for slender CNTs .

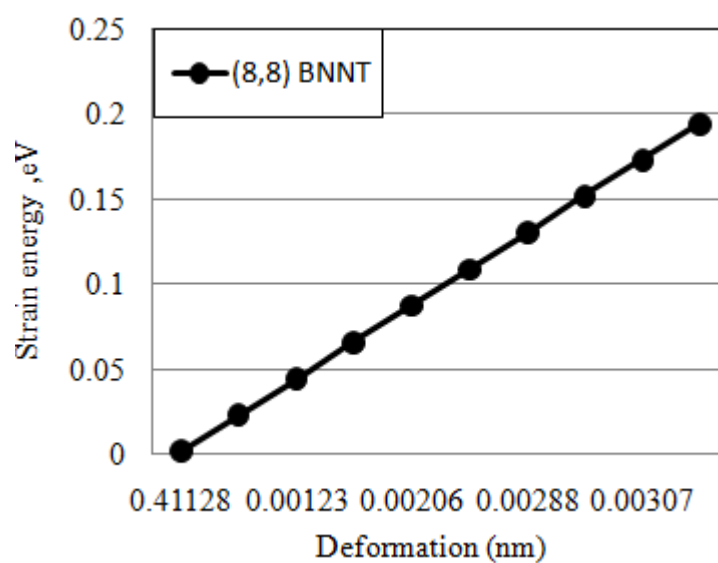


Figure 4.32: Strain energy v/s deformation profile for (8,8) BNNT

linearity was found when strain energy and deformations were plotted against each other and it results that buckling has said to have occurred for (8,8) BNNT.

(13,0) zigzag CNT

Buckling is defined to have occurred when there is a sudden drop in axial load in the axial load . This sudden drop in compressive axial load is observed for all CNTs considered. The load corresponding to buckling is termed the critical load (P_{cr}), The critical buckling strain (ε_{cr}) is related to by $\Delta l, \Delta l, /l$, where is l the original length of the CNT . At the onset of buckling , localized regions of depression develop as a result of membrane buckling. Almost immediately after that, the localized depressions coalesce to an allround constriction, producing a flattened attened neck on the CNT. This is known as the shell buckling mode, reminiscent to the bifurcation buckling of cylindrical shells under axial load, This continuum approach can be valid for buckling of slender CNTs where the CNT buckles in a global beam buckling mode instead of undergoing local shell buckling. ,[17]



Figure 4.33: A (13,0) CNT model

CNT (13,0) was modeled in modelling software with parameters such as $E=1.06\text{TPa}$, $\mu=0.19$ and cylinder radius as 0.066nm with ends clamped and remote displacement load was applied axially .

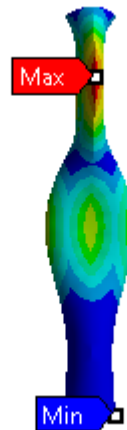


Figure 4.34: Eigen buckled deformation of (13,0) CNT

Table 4.25 represents the values of Euler buckling force and critical force computed and stresses and strains before and after FEM, which differentiates the buckling behaviour of nanotube. For FEM ultimate strengths and bilinear isotropic hardening factors were used for the non-linear buckling.

Chirality	diameter(nm)	$\frac{l}{d}$	F_{Euler} (nN)	Stress (σ)	Strain (ϵ)	Deformation(nm)
(13,0)	1.09	7.8508	13.88288	3890.6	0.0406	1.4142
			F_{cr} (nN)	Stress (σ_{cr})	Strain (ϵ_{cr})	Deformation(nm)
			0.86768009	899.9	0.0971	70.396

Table 4.25: Geometrical parameters and deformations after non-linear response

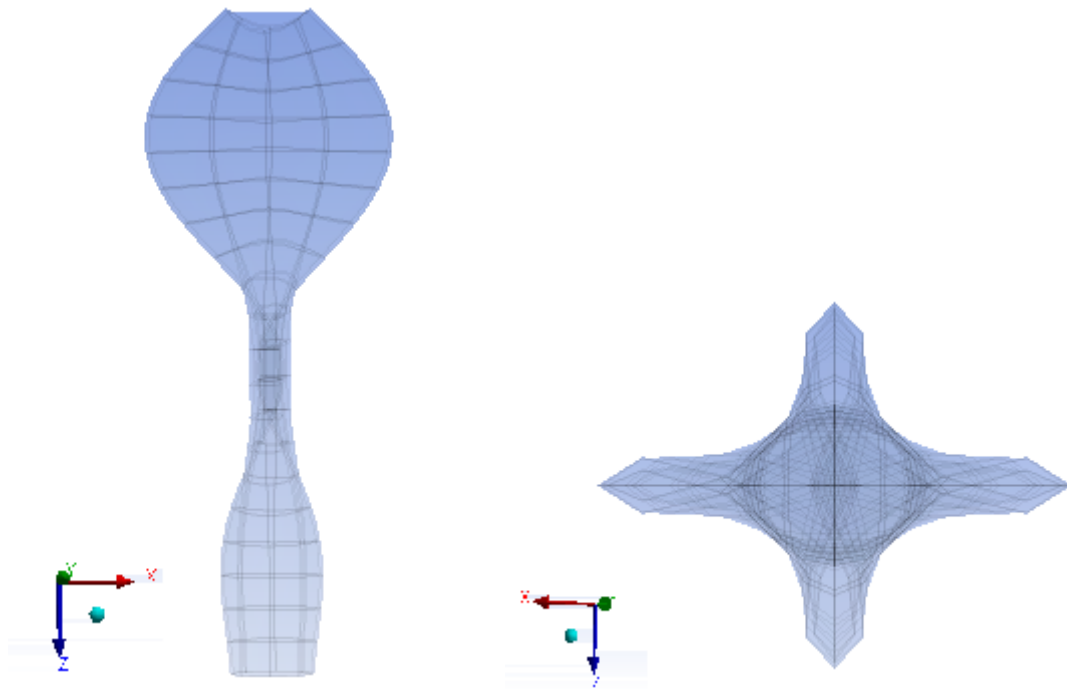


Figure 4.35: Buckled mode shape of CNT under compressive axial load

Two equilibrium structural configurations are possible from state of deformation.

After FEM and loads computed with the load multipliers the different morphological pattern of (13,0) CNT was represented in fig4.34



Figure 4.36: Buckled geometrical deformations after FEM eigen buckling analysis of (13,0) CNT

Chapter 5

Conclusions and future scope of work

5.1 conclusion

- The effects of tube chirality, elastic parameter and boundary condition on the critical compressive force of SWCNT and SWBNNT investigated because the buckling forces are sensitive to the tube chirality and end condition chosen for the analytical and simulated work.
- Overall results indicated that when aspect ratio is increasing the critical buckling forces of SWCNT and SWBNNT was found to be decreasing but on comparison part the Zigzag turns out to have higher values than that of armchair CNT and BNNT.
- And For constant aspect ratio and increasing nanotube diameter the critical buckling force was found to have increasing trend. Therefore armchair CNT type of the Single Walled Nanotubes turns out to be stiffer than the armchair BNNT type, and can be preferable for the load compression members.
- The buckling load gets reduced as one transits from the local beam theories to the nonlocal beam theories. This reduction in the buckling strain (or load) is most pronounced when the rod is short and stocky and when the ends of the rod are clamped.
- when the length of nanotube is very small , the buckling load is comparatively high and with the further increase of nanotube length, the buckling mode is changed into the Euler buckling mode of beam which leads to the lower buckling loads.
- Critical buckling strains were computed analytically and simulated with results that they are also not only sensitive to the constrained boundary condition but also to the tube chirality.

- Armchair CNT have higher critical buckling strain than BNNT . Therefore armchair boron nitride nanotubes can be preferable over CNTs as a compression members.
- The results indicates that the reduction of compressive strain due to the clamped boundary condition is relatively found to be dependent on tube diameter.
- And, It can also be predicted that the tube diameters mentioned have relatively small l_0/r and nanotubes can exhibit shell-like buckling behavior .
- An important observation of SWNTs with small aspect ratio is that they do not bend with respect to the tube axis and maintain their axis of symmetry .
- Using FSDST for different configurations armchair and zigzag and boundary conditions it was obseved that for smaller aspect ratios - short CNTs buckle in a shell mode .
- For, intermediated aspect ratios Nanotubes buckles in a flexural mode .
- And for large aspect raios - Slender Carbon nanotubes buckles globally in a flexural mode.
- Through non-linear responses it was observed that critical buckling force and strain of SWCNT ans SWBNNT varies with respect to the chirality of the tube .
- The critical buckling strains and forces for zigzag SWCNT was found to be higher than armchair CNT.

5.2 Future Scope

- Exploration of application based on buckling .
- Simulation for piezoelectric property estimation especially for BNNT.

Bibliography

- [1] Sumio Iijima et al. Helical microtubules of graphitic carbon. *nature*, 354(6348):56–58, 1991.
- [2] Angel Rubio, Jennifer L Corkill, and Marvin L Cohen. Theory of graphitic boron nitride nanotubes. *Physical Review B*, 49(7):5081, 1994.
- [3] Nasreen G Chopra, RJ Luyken, K Cherrey, Vincent H Crespi, et al. Boron nitride nanotubes. *Science*, 269(5226):966, 1995.
- [4] B Arash and Q Wang. A review on the application of nonlocal elastic models in modeling of carbon nanotubes and graphenes. *Computational materials science*, 51(1):303–313, 2012.
- [5] J Bernholc, C Brabec, M Buongiorno Nardelli, A Maiti, C Roland, and BI Yakobson. Theory of growth and mechanical properties of nanotubes. *Applied Physics A: Materials Science & Processing*, 67(1):39–46, 1998.
- [6] Michael R Falvo, GJ Clary, RM Taylor, V Chi, Frederick Phillips Brooks, Sean Washburn, and Richard Superfine. Bending and buckling of carbon nanotubes under large strain. *Nature*, 389(6651):582–584, 1997.
- [7] James A Elliott, Jan KW Sandler, Alan H Windle, Robert J Young, and Milo SP Shaffer. Collapse of single-wall carbon nanotubes is diameter dependent. *Physical Review Letters*, 92(9):095501, 2004.
- [8] Guoxin Cao and XI Chen. The effects of chirality and boundary conditions on the mechanical properties of single-walled carbon nanotubes. *International Journal of Solids and Structures*, 44(17):5447–5465, 2007.
- [9] Antonio Pantano, David M Parks, and Mary C Boyce. Mechanics of deformation of single-and multi-wall carbon nanotubes. *Journal of the Mechanics and Physics of Solids*, 52(4):789–821, 2004.
- [10] Boris I Yakobson, CJ Brabec, and J Bernholc. Nanomechanics of carbon tubes: instabilities beyond linear response. *Physical review letters*, 76(14):2511, 1996.

- [11] N Hu, K Nunoya, D Pan, T Okabe, and H Fukunaga. Prediction of buckling characteristics of carbon nanotubes. *International Journal of Solids and Structures*, 44(20):6535–6550, 2007.
- [12] Chunyu Li and Tsu-Wei Chou. A structural mechanics approach for the analysis of carbon nanotubes. *International Journal of Solids and Structures*, 40(10):2487–2499, 2003.
- [13] Yonggang Huang, J Wu, and Keh-Chih Hwang. Thickness of graphene and single-wall carbon nanotubes. *Physical review B*, 74(24):245413, 2006.
- [14] Sumio Iijima, Charles Brabec, Amitesh Maiti, and Jerzy Bernholc. Structural flexibility of carbon nanotubes. *The Journal of chemical physics*, 104(5):2089–2092, 1996.
- [15] Guoxin Cao and Xi Chen. Buckling of single-walled carbon nanotubes upon bending: Molecular dynamics simulations and finite element method. *Physical Review B*, 73(15):155435, 2006.
- [16] Amar Nath Roy Chowdhury, Chien Ming Wang, and Soo Jin Adrian Koh. Continuum shell model for buckling of single-walled carbon nanotubes with different chiral angles. *International Journal of Structural Stability and Dynamics*, 14(04):1450006, 2014.
- [17] Xiaohu Yao, Qiang Han, and Hao Xin. Bending buckling behaviors of single-and multi-walled carbon nanotubes. *Computational Materials Science*, 43(4):579–590, 2008.
- [18] T Belytschko, SP Xiao, George C Schatz, and RS Ruoff. Atomistic simulations of nanotube fracture. *Physical Review B*, 65(23):235430, 2002.
- [19] Chunyu Li and Tsu-Wei Chou. Modeling of elastic buckling of carbon nanotubes by molecular structural mechanics approach. *Mechanics of Materials*, 36(11):1047–1055, 2004.
- [20] K Yazdchi, M Salehi, and MM Shokrieh. Effective structural parameters of single-walled carbon nanotubes. *The European Society for Composite Materials*, pages 1–10, 2008.
- [21] Markus J Buehler, Yong Kong, and Huajian Gao. Deformation mechanisms of very long single-wall carbon nanotubes subject to compressive loading. *Journal of Engineering Materials and Technology*, 126(3):245–249, 2004.
- [22] Xuekun Sun and Wenming Zhao. Prediction of stiffness and strength of single-walled carbon nanotubes by molecular-mechanics based finite element approach. *Materials Science and Engineering: A*, 390(1):366–371, 2005.

- [23] KI Tserpes and P Papanikos. Finite element modeling of single-walled carbon nanotubes. *Composites Part B: Engineering*, 36(5):468–477, 2005.
- [24] Mogurampelly Santosh, Prabal K Maiti, and AK Sood. Elastic properties of boron nitride nanotubes and their comparison with carbon nanotubes. *Journal of nanoscience and nanotechnology*, 9(9):5425–5430, 2009.
- [25] Roham Rafiee and Reza Maleki Moghadam. On the modeling of carbon nanotubes: a critical review. *Composites Part B: Engineering*, 56:435–449, 2014.
- [26] GI Giannopoulos, AP Tsiros, and SK Georgantzinou. Prediction of elastic mechanical behavior and stability of single-walled carbon nanotubes using bar elements. *Mechanics of Advanced Materials and Structures*, 20(9):730–741, 2013.
- [27] MS Dresselhaus, G Dresselhaus, and R Saito. Physics of carbon nanotubes. *Carbon*, 33(7):883–891, 1995.
- [28] Anthony K Rappé, Carla J Casewit, KS Colwell, WA Goddard Iii, and WM Skiff. Uff, a full periodic table force field for molecular mechanics and molecular dynamics simulations. *Journal of the American chemical society*, 114(25):10024–10035, 1992.
- [29] Ali Ghavamian, Moones Rahmandoust, and Andreas Öchsner. On the determination of the shear modulus of carbon nanotubes. *Composites Part B: Engineering*, 44(1):52–59, 2013.
- [30] Jian Ping Lu. Elastic properties of carbon nanotubes and nanoropes. *Physical Review Letters*, 79(7):1297, 1997.
- [31] CM Wang, YY Zhang, Sai Sudha Ramesh, and S Kitipornchai. Buckling analysis of micro-and nano-rods/tubes based on nonlocal timoshenko beam theory. *Journal of Physics D: Applied Physics*, 39(17):3904, 2006.
- [32] Mitesh B Panchal, SH Upadhyay, and SP Harsha. Mass detection using single walled boron nitride nanotube as a nanomechanical resonator. *Nano*, 7(04):1250029, 2012.
- [33] Mitesh B Panchal and SH Upadhyay. Cantilevered single walled boron nitride nanotube based nanomechanical resonators of zigzag and armchair forms. *Physica E: Low-dimensional Systems and Nanostructures*, 50:73–82, 2013.
- [34] Mitesh B Panchal, SH Upadhyay, and SP Harsha. Vibration analysis of single walled boron nitride nanotube based nanoresonators. *Journal of Nanotechnology in Engineering and Medicine*, 3(3):031004, 2012.